Title
I. STUDIES IN NUCLEAR REACTIONS INDUCED BY HIGH ENERGY X-RAYS. II. NUCLEAR ISOMERISM IN Co58

Author
Strauch, Karl

Publication Date
1950-05-19

COPY 2

UCRL 708

I. Studies in Nuclear Reactions Induced by High Energy X-Rays

II. Nuclear Isomerism in Co^{58}

by

Karl Strauch
A.B. (University of California) 1943

UNCLASSIFIED

DISSERTATION

Submitted in partial satisfaction of the requirements for the degree of

DOCTOR OF PHILOSOPHY

in

Physics

in the

GRADUATE DIVISION

of the

UNIVERSITY OF CALIFORNIA

Approved: . . . . . .

. . . . . .

. . . . . .

Committee in Charge

Deposited in the University Library . . . . . .
Date Librarian

DISCLAIMER

I. Studies in Nuclear Reactions Induced by High Energy X-Rays

TABLE OF CONTENTS

TABLE OF CONTENTS (Cont.)

A. INTRODUCTION

The subject of x-ray induced nuclear reactions started with the photodisintegration of deuterium[1] and beryllium[2] with γ-rays emitted by the naturally occurring radioactive isotopes ThC" and RaC. The low energies (2.6 Mev and 2.4 Mev) available from these two sources are insufficient to eject a nucleon from the vast majority of nuclei. Bothe and Gentner[3,4] used the more energetic γ-rays produced in the reactions $B^{11}(p,\gamma)C^{12}$ (11.8 Mev) and $Li^{7}(p,\gamma)Be^{8}$ (17.5 Mev) to eject one neutron from many isotopes: their relative yield measurements and absolute cross section determination represent the first quantitative data on the energy dependence of the nuclear photoeffect. Several groups of investigators have been and are active in this field: the results of Wäffler et al. as reported in a series of papers[5,6] represent a rather complete investigation of (γ,n) and (γ,p) processes with the Li γ-ray.

In order to study photon induced reactions resulting in the ejection of more than one nucleon higher x-ray energies are in general required: these became available in the bremsstrahlung emitted by accelerated high energy electrons. The General Electric betatron x-ray beam with a maximum energy of 100 Mev made possible the relative yield measurements of many reactions by Perlman and Friedlander,[7] the absolute cross section measurement of Lawson,[8] the excitation curve determinations of Baldwin and Klaiber.[9] Accurate threshold values were obtained by McElhinney et al.[10] for several (γ,n) and (γ,p) reactions, and yields and angular distributions of some (γ,n) processes were measured by Price and Kerst[11] using the Illinois 21 Mev betatron.

To understand the mechanism of photonuclear reactions it is of interest to know the cross sections of the different types of reaction and the energy

of the photons responsible. The work of the General Electric group previously referred to gives some information on these points: their data leaves doubtful the role of competing reactions in the nuclear photoeffect. The use of a bremsstrahlung spectrum complicates such experiments. The shape of this spectrum for a maximum energy of 330 Mev after correction for target thickness is of the form:

$$\phi(v,U) = \frac{t}{2} \frac{1}{v} \left\{ \mu(W) - \ln(1 - v) \right\} \qquad (1)$$

where $v = \frac{W}{U} = \frac{W}{330} = \frac{\text{photon energy}}{\text{energy of primary electron}}$

$\mu(W)$ = absorption coefficient per shower unit of photon of energy W

$\phi(v,U)$ = probability of an electron of energy U to emit a photon of fractional energy v per unit thickness of material. This function is tabulated in Rossi and Greisen:[12] its asymptotic form at large energies is $\phi(v) = 1/v$.

Thus all x-ray energies are present in the beam in varying amounts as indicated in this equation: to obtain relative cross sections for various reactions some information concerning their energy dependence is therefore required.

The excitation functions of Baldwin and Klaiber were obtained with the 100 Mev betatron by varying the maximum energy of the beam and normalizing the beam intensity at various energies with the help of a calculated energy response of the monitor. With the completion of the Berkeley 330 Mev synchrotron another approach to this problem became possible. Due to the high energy photons present in the x-ray beam cascade processes became important as the beam passes through an absorber such as lead. By studying the intensity variation in the lead of these x-rays responsible for a given nuclear reaction, it is possible to determine the mean energy of these photons

using the well established shower theory. Some information on the energy spread of these "effective photons" can also be obtained.

This method will be studied and applied to several photonuclear reactions in part B of this paper; relative and absolute cross section measurements will be reported in part C and some conclusions concerning the mechanism of these reactions will be examined in part D.

B. TRANSITION CURVES

1. Introduction. As a high energy electron passes through matter it loses energy by radiative collisions: on the average it loses 1/e of its original energy in about .40 cm of Pb. A large fraction of this energy is emitted in the form of quanta of energy comparable to the initial energy.[13] A high energy photon is primarily absorbed by pair creation; the mean free path for this process is about .65 cm of Pb and on the average the photon energy is equally shared among the two electrons.[13] Thus as a high energy photon passes through lead, it produces a pair, each member of which in turn emits a quantum which then produces pairs and the process repeats itself until a low "critical energy" (7 Mev for Pb) is reached where the pair production and radiation cross sections become small and of the order of the cross sections for other methods of energy loss. This is the well known cascade shower process the development of which is usually described in terms of a unit of length called the "radiation length" or "shower unit": its value for Pb is 5.9 gr/cm^2 or .53 cm which is the average of the mean free paths for pair production and radiation emission.

As the synchrotron bremsstrahlen with a maximum energy of 330 Mev pass through an absorber such as lead, their spectral composition changes as they penetrate the material: high energy photons disappear, lower energy photons multiply. This multiplication becomes the more important, the lower the energy of the photons under consideration. To study this effect, detectors sensitive to various photon energies are needed: these are available in the form of photonuclear reactions with various thresholds. When an element is placed in the synchrotron beam, different photon induced reactions occur resulting in the ejection of one or more particles from the target nucleus. The reaction is determined by the known target and product nuclei: the latter are identified

by their known half-lives when unstable. A reaction resulting in the production of a stable isotope is of course not observed by this method. The amount of activity in the target is proportional to the number of photons incident that are effective in producing the reaction under study: by thus placing identical targets at various depths of lead and comparing their activity, the density of "effective photons" is measured as a function of lead thickness. The resulting density curve is similar to the transition curves or Rossi curves obtained in cosmic ray work, only here the transformation in lead of a selected energy range of x-rays, the range of "effective photons" is being studied.

Experiments leading to several transition curves will now be described: first a description of the experimental set-up will be given, then results with (γ,n) reactions on C, Cu and Ag as detectors will be presented; these will be compared with the predictions of the cascade shower theory and other experiments, and finally results from various other reactions will be shown.

2. Experimental set-up. A stack of lead absorbers 9 x 9 inches in area is placed at 5 1/3 feet from the synchrotron platinum target (Figure 1). The stack is centered on the beam by the use of a photographically aligned telescope. Foils of the target material have an area of 3 3/4 x 3 3/4 inches and a thickness determined by the activity required for counting purposes. They are mounted on thin cardboard holders and placed at various depths in the lead stack. This is the standard set-up and is designated Geometry 1 (Figure 1). The thickness of the lead absorbers is determined by weight and area measurements: the resulting value in gr/cm^2 is then divided by 5.9 to obtain the thickness in shower units (s.u.). The sample foils are cut to size with a tolerance of 1/100 inch and weighed: foils of similar weight are then selected for comparison.

When a transition curve is being measured that uses as detector a reaction resulting in a short half-life such as $Cu^{63}(\gamma,n)Cu^{62}$ 10.1 minutes a monitor foil is placed in front of the absorber stack, and one or two foils are placed inside during a run. If a longer half-life results from the reaction under study such as $Zn^{64}(\gamma,n)Zn^{62}$ 9.5 hours a complete set of 24 foils is placed inside the absorber stack during the irradiation. After bombardment with the synchrotron beam the foils are rolled into cylinders having a diameter of 7/8 inches, placed over Eck and Krebs thin walled glass Geiger counters, and their activities compared. The consecutive interchange of samples compensates for the different counter efficiencies. The bombardment time depends of course on the half-life and the yield of the product nucleus, but is in general of the same order as the half-life. For instance, a 14 mil Cu foil of standard size placed for 2 minutes in an average beam will give about 4000 counts per minute.

The Geometry 1 just described was chosen so as to include most of the scattered beam as it progresses through Pb; detailed tests described in the next section indicate that the transition curves obtained with this geometry would not be changed by using larger absorbers or detectors.

3. Results with C, Cu, and Ag detectors using 330 Mev bremsstrahlung. Bombardment of polystyrene yields the 20.1 minute activity due to the reaction $C^{12}(\gamma,n)C^{11}$. No other half-life appeared for as long as the sample could be counted. Irradiation of several minutes of Cu metal produced the 10.1 minute activity resulting from the reaction $Cu^{63}(\gamma,n)Cu^{62}$; for at least five half-lives no other activity is evident. In part C of this paper it is shown that the $(\gamma,3n)$ yield is at least 25 times smaller than the (γ,n) yield in the case of Zn; there is no reason to suppose that the reaction $Cu^{65}(\gamma,3n)Cu^{62}$ contributes appreciably to the 10.1 minute activity. Ag metal when bombarded

for about 15 minutes contains the 2.3 and 24 minute activities due to the reactions $Ag^{109}(\gamma,n)Ag^{108}$ and $Ag^{107}(\gamma,n)Ag^{106}$ respectively, besides small amounts (low counting efficiencies) of the 40 second isomers of the two stable isotopes. By waiting 12 minutes before starting the count, only the 24 minute product was observed.

Using the Geometry 1 previously described transition curves using these three (γ,n) reactions have been obtained and the results are plotted in Figure 2: the activity of the monitor foil is arbitrarily set at 1.0 and the depth in lead is expressed in shower units. The foil thicknesses were: polystyrene 16 mils (.001 s.u.); copper 14 mils (.024 s.u.); silver 2 mils (.005 s.u.). Only at the very beginning of the curve obtained with Cu detectors are these lengths comparable to the absorber thickness: in this case the depth of the position of the detector foil was obtained by adding the thickness in shower units of Pb and Cu.

The three transition curves show the same characteristic features: (1) an initial drop due to photon absorption followed (2) by a region in which multiplication by the cascade process of the "effective photons" results in a maximum; (3) at larger depths an exponential absorption is approached. The last feature becomes more apparent in Figure 3 which is plotted on semi-logarithmic paper. The three curves will be examined in more detail in sections 5 and 6 where it will be shown that the average photon energies responsible for the (γ,n) reactions on C, Cu and Ag are 30 Mev, 20 Mev and 18 Mev respectively.

The beginning of the transition curves are of particular interest for the theoretical interpretation: Figure 4 shows this as obtained with 16 mil (.001 s.u.) polystyrene and 2 mil (.004 s.u.) Cu foils. The indicated uncertainties are standard deviations obtained from the number of counts taken. It is seen that the dip of the $Cu^{63}(\gamma,n)Cu^{62}$ curve is only 4 times the size of the

standard deviation, and as a result this section of the curve was not obtained with high accuracy. For the $C^{12}(\gamma,n)C^{11}$ curve the dip is more pronounced, and is of the order of 9 times the minimum standard deviation: here however inhomogeneities in the polystyrene available introduced an additional uncertainty.

As the x-ray beam passes through the lead stack, not only does its spectral composition change, but it also spreads in a lateral direction due to the finite angle of emission of electrons and photons, and multiple scattering of electrons. This later factor is the dominant one; the root mean square angle of scattering in 1 radiation length of electrons of energy E in Mev is of the order of 21/E radians.[12] Thus the higher the energies under study, the smaller the scattering becomes. As will be seen later we are selecting photon energies of 18 Mev or higher: Roberg and Nordheim[14] have calculated the angular and lateral spread of photons in high energy showers: they obtain in lead for 18 Mev photons a root mean square angular spread of 0.4 radians and a root mean square lateral spread of 0.98 shower units. Although the sizes of absorbers and detectors in Geometry 1 should be large enough to take this scattering into account, several experimental tests were made to verify this conclusion since the quantitative interpretation of the transition curves depends on the applicability of one dimensional shower theory. The following tests were made using Cu detectors in general since these are sensitive to lower energy x-rays for which geometrical effects are most pronounced:

(1) The shape of the synchrotron beam was determined at the position of the lead stack by comparing the activities of Cu disks of 1/4 inch diameter placed at various distances from the center of the beam. This was done both in front and behind 2.7 s.u. of lead (the region of highest "effective photon" density), the results being shown in Figure 5. Since the activity of the disks

off the axis is low, the measurement is not very sensitive to a small spreading effect; however it shows that the effect cannot be large.

(2) The activity induced in the 3 3/4 x 3 3/4 detector foils is not entirely used: the counter sensitivity limits the effective foil width to 3 inches as shown by the sensitivity plot (lower curve on Figure 5) of the thin wall counters used. The counting effect of another foil edge is reduced by the larger self-absorption resulting from a certain amount of overlapping when the foils are wrapped into cylinders. However using 2 mil and 16 mil Cu foils the same height of the maximum is observed (Figure 8): this is to be expected as the activity near the edge is small and the self-absorption for 16 mils of Cu is less than 20 percent. The usable size of the detector foils is thus 3 3/4 x 3 inches.

(3) The transition curves for the (γ,n) reactions in C and Cu as detectors were taken using lead absorbers of area 2 1/2 x 3 1/2 inches and detector disks of 1 5/8 inches diameter: this is Geometry 2 in Figure 1. Standard end window Victoreen tubes were used to compare the activities: since their counting efficiencies decrease rapidly off the central axis, the effective size of the detector disks is smaller than the geometrical one. Geometry 2 is thus smaller by about a factor of 3 than the standard Geometry 1. The experimental points with polystyrene detectors are shown in Figure 6; there is no difference between the results with the two geometries, and both sets are used to obtain the transition curve for this case. Figure 7 shows the transition curve obtained with Cu detectors under Geometry 1; points obtained with Geometry 2 are seen to lie about 5 percent below the curve. This difference in behavior with the two detectors is not suprising, since lower energy photons are effective in producing the copper activity and these are scattered more than the higher energy quanta responsible for the C reaction. The large

difference in size of both detectors and absorbers in Geometry 1 and 2 and the small difference in results in the case of copper only indicates that the transition curves would not be changed appreciably by using a still larger geometry.

(4) A direct test of this conclusion is afforded by the use of Geometry 3 (see Figure 1): here monitor and detector foils are placed above their normal position so as to be irradiated by the portion of the beam not usually used. Only about 1 percent of the total beam is incident on Geometry 3: most of the x-rays pass below it. Thus if scattering outside the normal set-up is important, far more "effective photons" will scatter into Geometry 3 than out of it resulting in a higher maximum than that obtained under normal conditions. If this scattering is unimportant however, then the peak should be lower since we are using the side band of the synchrotron beam which contains fewer high energy quanta resulting in a decreased cascade effect.

Experimental results obtained with 12 mil Cu foils and Geometry 3 are shown by the lower curve in Figure 7. The ratio of activities of monitor foils in Geometries 3 and 1 is .012 as determined by comparing at the same time 12 mil and 1 mil foils placed in the respective set-ups so as not to overload the counters. This transition curve has a lower peak than under normal conditions as expected in the case of no or very small scattering effect; at larger depths the curve appears to decrease less than normal: this is probably due to the neutron background appreciable at these low intensities. If we take the worst case and assume this broadening to be entirely due to scattered photons, we can use this result to correct the transition curve obtained under normal conditions for the portion of the beam missing the detectors and the maximum possible number of scattered photons. These corrected points are indicated as crosses on Figure 7: they were obtained by

adding to the transition curve from Geometry 1 eight times (solid angle correction) the transition curve from Geometry 3 and normalizing the 0 absorber point to 1.00. The correction for each point amounts to 1 percent or less and can be neglected in comparison with other sources of error.

(5) Another way to estimate the influence of scattered photons is to collimate the x-ray beam before it hits the absorber stack so that only scattered photons reach the foils placed in Geometry 3. This was tried with the 1 inch collimator placed 5 feet from the platinum target; the resulting activities were so small as to be entirely explained by the increased neutron background from the collimator and no effect due to scattered photons could be detected.

(6) The tests described so far are mostly sensitive to the lateral spread of quanta in the lead absorbers. The angular scattering of the "effective photons" is expected to be small as seen above, however since backscattering in the absorber is not taken into account in the theory used to interpret the transition curves, an attempt was made to detect such an effect. 16 mil Cu foils were used in Geometry 1: the detector activity with lead backing y_{Pb} was compared to the activity with no backing y_o. This was done at various absorber depths and the results are shown in the upper plot of Figure 8: it is seen that no backscattering effect could be observed.

(7) To determine whether the size of the beam had any influence on the shape of the transition curve, a collimator was placed 5 feet from the platinum target, just in front of the absorber stack of Geometry 1. The height of the curve obtained with Cu detectors at 2.7 shower units did not change appreciably when 2, 1, 1/2 and 1/4 inch openings were used as seen on the lower plot of Figure 7.

Considering the tests just described it appears safe to conclude that the transition curves obtained with Geometry 1 are not affected by the set-up chosen. The results include most all of the scattered photons and are not affected by backscattering. Thus the one-dimensional shower theory can be applied in the interpretation of the observed curves.

4. Results with C and Cu detectors using 200 Mev bremsstrahlung. The maximum beam energy was reduced to about 200 Mev and transition curves taken with C and Cu detectors placed in the standard Geometry 1. The results are plotted in Figure 9 and 10: the maximum beam energy used in the case of polystyrene detectors was 210 ± 5 Mev and 206 ± 5 Mev in the case of Cu foils. The error in the energies was estimated from the repeatability of the required machine adjustments and assumes a normal maximum beam energy of 330 Mev. Figure 8 and 9 also show the curves obtained with the 330 Mev beam for comparison: general features are the same for both sets of data. Multiplication plays a smaller part when the lower energy beam is used. These transition curves will be examined in more detail in the following section.

5. Characteristic features of transition curves. The transition curves presented in this paper are obtained by selecting from the synchrotron x-ray beam those "effective photons" responsible for certain nuclear reactions, and studying the changes in density of this particular group of quantum energies as the beam travels through lead. The reactions under study could also be produced by secondary neutrons or electrons originating in the synchrotron or lead stack. The first contribute in general less than 0.3 percent to the observed activities as shown by the shape of the transition curves at large depths. An exception is $Al^{27}(\gamma,n2p)Na^{24}$ where a large neutron background was observed: this is explained by the low threshold and large yield of the (n,α) reaction leading to the same end product. Laughlin et al.[15]

have measured the cross section for the reaction $Cu^{63}(e,e'n)Cu^{62}$ with 16 Mev electrons and obtained a value of 1.7×10^{-28} cm^2; this is to be compared to the cross section for $Cu^{63}(\gamma,n)Cu^{62}$ which is 1.2×10^{-25} cm^2 for 17 Mev x-rays.(6) Since the number of electrons and photons in the lead stack are of the same order of magnitude, only the quanta need to be considered in our study.

The detailed features of the observed transition curves will now be examined and then compared with predictions from the shower theory in sections 6 and 7. As the synchrotron beam starts to penetrate the lead stack, the "effective photons" are being absorbed due to pair production. In the region under consideration high energy photons are more rapidly absorbed in the lead than low energy quanta: the absorption coefficient as obtained from the initial drop should correspond to the value for the highest energy x-ray participating in the reaction. As seen in section 4 this is hard to measure experimentally since very small thicknesses of lead and small intensity changes are involved. However any sizable contributions from x-rays with energies appreciably different from the average would show up most strongly in this region.

At larger depths multiplication of the photons responsible for the reactions becomes important due to showers initiated by the very high energy x-rays present in the beam. The lower the energy of the photons being observed, the more multiplication becomes important: this results in a higher peak reached at a larger depth of lead as shown clearly in Figure 2. The photons responsible for the $Ag^{107}(\gamma,n)Ag^{106}$ reaction are on the average of lower energy than those effective in $Cu^{63}(\gamma,n)Cu^{62}$; $C^{12}(\gamma,n)C^{11}$ is produced by still higher energy quanta. When the maximum energy of the incident beam is reduced, multiplication becomes less prominent as seen on Figures 9 and 10.

After the peak has been passed, cascade effects become rapidly less important since the high energy quanta have been mainly absorbed (the mean free

path of a 330 Mev photon in Pb is 1.1 s.u.); only the most penetrating photons are still effective in producing the observed reaction. This means the transition curves in this region tend to an exponential decrease, and the lower the x-ray energy the deeper in the lead is this state reached (see Figure 3). The slope of the exponential decrease should tend to the value corresponding to the lowest energy "effective photon," that is a quantum of threshold energy. Actually this state was not reached in these experiments since due to the small cross sections near the threshold it occurs at very large absorber depths where the induced activities are too small or where the contribution from neutron background becomes important. The transition curves for photons causing a particular reaction obtained with two different maximum beam energies have the same final slopes (Figure 10).

To summarize, the characteristic energy dependent features of a transition curve are:

(1) the initial drop - portion most sensitive to possible high energy photon contributions;

(2) the height and position of the maximum when such exists - produced by the average of all "effective photon" energies;

(3) the final slope - feature most sensitive to low energy x-ray contribution;

(4) the total area enclosed under each transition curve, called "track length" since it is proportional to the total distance travelled by all "effective photons."

Only features (2) and (4) can be measured accurately and for determination of photon energies the track length turns out to be the most useful characteristic for both experimental and theoretical reasons.

6. Average photon energy from track length. In order to obtain the average energy of the "effective photons" predictions from the theory of cascade processes are used. This theory was first developed independently by Carlson and Oppenheimer[16] and Bhabha and Heitler[17] and many contributions have since been published. A comprehensive treatment is given by Rossi and Greisen[12] whose notation will be used here. We are primarily interested in two functions:

$\Upsilon(W_o,W,t)dW$ the average number of photons at the thickness t with energy between W and W+dW in a shower initiated by a photon of energy W_o

$z_\gamma(W_o,W) = \int_o^\infty \Upsilon(W_o,W,t)\,dt$ the total distance travelled by photons of energy W in a shower produced by a quantum of energy W_o.

Since the incident bremsstrahlung is known from equation (1) a solution for $\Upsilon(W_o,W,t)dW$ would determine the shape of the transition curve for a particular photon energy W while a solution for $z_\gamma(W_o,W)$ would give the area or track length of this curve. An exact mathematical treatment cannot be carried out; Rossi and Greisen under "Approximation B" carry out the calculations using asymptotic formulae for radiation processes and pair production, assuming a constant collision loss for electrons and neglecting Compton effect.

For the case of 330 Mev bremsstrahlung these results are unsatisfactory since at and below this energy the pair production and radiation cross sections are markedly different from the asymptotic values. Eyges[18] has made modifications for this case and obtains:

$$z_{rel}(W_o,W) = \frac{.38}{\mu(W)}\,\frac{W_o}{W}\,\frac{1}{\left\{1 + .78\left(\frac{\beta}{W}\right) - .29\left(\frac{\beta}{W}\right)^2 + \ldots\right\}\left\{\frac{4}{3}\left(1 - \frac{W}{W_o}\right)\right\}} \qquad (2)$$

where $z_{rel}(W_o,W)$ = normalized track length of photons

W_o = maximum energy of the bremsstrahlung

W = energy of the photon under consideration

β = critical energy for Pb = 7 Mev

$\mu(W)$ = total absorption coefficient per radiation length at W

The constant factor of 0.38 comes from using not the asymptotic value of the radiation probability but a suitable average for the energy region of interest; this factor also includes the influence of the incident bremsstrahlung spectrum. The expression in brackets originates from the normalization of differential photon spectrum at zero absorber thickness. The expansion in $\frac{\beta}{W}$ corrects for the ionization loss of the electrons. The use of the total absorption coefficient introduces some correction for the Compton effect.

The numerical values of $\mu(W)$ are obtained by drawing a smooth curve through the theoretical values listed by Heitler[13] after a 10 percent reduction has been applied: this correction is needed so that the experimental absorption coefficients as obtained by Walker at 17.6 Mev[19] and Lawson at 88 Mev[20] fall on the curve to be used.

The track length of the observed curves then determines an average photon energy W_{av} responsible for the reactions under study and the values thus obtained are shown in Table III. The experiments of Baldwin and Klaiber[9] give for the energies at which the peak of the cross sections occur values of 22 Mev for $Cu^{63}(\gamma,n)Cu^{62}$ and 30 Mev for $C^{12}(\gamma,n)C^{11}$; these are in good agreement with the transition curve method from which average photon energies of 20 Mev and 30 Mev are obtained for these reactions.

In order to estimate the dependence of the experimental average photon energy on the energy range of the "effective photons" the following calculation was carried out: a W_{av} was assumed and then postulated that photons in an energy interval of $\frac{1}{2}W_{av}$ contribute equally to the observed activities; the track lengths for various energies in this interval were then obtained from

formula (2) and the average of these taken. This average track length determined an energy whose value differed by three percent or less from the original W_{av} between 20 Mev and 100 Mev.

A very accurate theoretical expression can be obtained for the ratio of track lengths of two transition curves for the same photon energies but different maximum bremsstrahlung energies:

$$\frac{z_{rel}(W,W_o^1)}{z_{rel}(W,W_o^2)} = \frac{W_o^1}{W_o^2} \frac{(1 - W/W_o^2)}{(1 - W/W_o^1)} \qquad (3)$$

where W_o^1 = maximum beam energy used for transition curve 1

W_o^2 = maximum beam energy used for transition curve 2

W = photon energy under investigation

As can be seen most approximations have been eliminated from this expression and W appears only in the correction terms. Table I lists the experimental results for the (γ,n) reactions on C and Cu, and the theoretical results obtained from (3): the agreement is seen to be good. It may be concluded that the average "effective photon" energy W_{av} obtained from the track length of the experimental transition curves by the use of expression (2) should be reliable both because the area under the curves can be obtained accurately, and because formula (2) involves few approximation and is insensitive to the energy spread of the "effective photons."

7. Energy range of "effective photons." As was pointed out in section 5 the detailed shape of the transition curves is sensitive to the energy spread of the "effective photons." Conclusions obtained from this feature are subject to serious limitations however:

(1) Theoretical calculations can only be carried out with several approximations which become less reliable as the photon energy decreases.

(2) The bremsstrahlung spectrum of the incident beam greatly reduces the

apparent effect of high energy photons.

In the case of (γ,n) reactions, in particular for Cu and C, independent evidence exists which indicates that the energies of the "effective photons" are grouped quite closely around an average value; it appears that a good procedure would consist in seeing how this conclusion is verified by the shape of the corresponding transition curves, and then compare to these the shape of the transition curves for other reactions.

The main support for the small width of photon energies responsible for (γ,n) reactions comes from:

(1) The relative yields of the many (γ,n) reactions measured by Perlman and Friedlander[7] are the same using maximum beam energies of 50 Mev and 100 Mev. Several of these were also measured with 330 Mev maximum beam energies as shown in Table II and the same relative values are again obtained. This means either that the excitation functions for these reactions are all similar, or that no significant contributions occur from photons beyond 50 Mev.

(2) Baldwin and Klaiber[9] have measured the excitation functions of the reactions $C^{12}(\gamma,n)C^{11}$ and $Cu^{63}(\gamma,n)Cu^{62}$: they obtain very sharp peaks at 30 Mev and 22 Mev respectively. Their experiment required the theoretically calculated energy response of the beam monitor which is open to some argument, and also a differentiation of the experimental curve; this leads to some question about the reliability of the details of the observed shape. McElhinney et al.[10] have measured excitation functions for $Ta^{181}(\gamma,n)Ta^{180}$ and one half of the curve for $Cu^{63}(\gamma,n)Cu^{62}$ by a similar method: their results also show a resonance peak although of larger half-width.

(3) The cross section for the reaction $Cu^{63}(\gamma,n)Cu^{62}$ at 17.5 Mev has been measured by Wäffler[6] and found to be 1.2×10^{-25} cm^2. The integrated cross section $\bar{\sigma} = \int_{W_{min}}^{W_{max}} \sigma(W)dW$ for this reaction has been measured by

Lawson[8] with 100 Mev bremsstrahlung and as reported in part C with 330 Mev maximum energy: an average value of 1.2 Mev-barns was obtained. Taking the cross section peak at 20 Mev and assuming as a first approximation a triangular shape for the excitation curve, a 3 Mev width at half maximum is obtained.

(4) As seen in the previous section, the ratio of track lengths of the transition curves taken with 330 Mev and 200 Mev beams for the photons causing (γ,n) reactions on Cu and C checks the theoretical value obtained by assuming that no contribution from photons between 200 Mev and 330 Mev occurs.

What does the detailed shape of the transition curves show? For distances of less than 1 shower unit the curves can be calculated with good accuracy as first pointed out by Serber.[21] The calculation has been carried out by Eyges for 20 Mev and 30 Mev photons and his results are plotted in Figure 4. It is apparent that the experimental points lie if anything slightly above the theoretical curves. The relatively large difference between the two calculated curves shows the sensitivity of this region to high energy photons, and none are observed.

At larger distances the theoretical solutions become less reliable: beyond about 10 shower units they become very sensitive to the values of $\mu(W)$; this is not important for the track length since contributions to the area become small, but it shows up in the detailed shape. Eyges has calculated the detailed transition curves for 20 Mev and 30 Mev photons and his results are shown by the dotted lines in Figures 6 and 7. It is apparent that the agreement with experimental points is excellent for the case of 30 Mev photons; a slight discrepancy appears only at large depths of lead which is not suprising as just noted. For 20 Mev photons the check with experiment is not as good: the theoretical curve is too low below 3 shower units, too

high at the end. This relative behavior is expected since the track length must check the experimental one. The reason for the discrepancy probably lies in the low value of the average photon energy: it is only three times the "critical energy" and the correction for ionization loss might become unreliable. The Compton cross section also contributes 10 percent to the total absorption in this region. The failure of the two curves to agree cannot be explained by contributions of photon energies much different from 20 Mev: this would lower the experimental curve at small distances, raise it at large depths.

The final slope appears as the most sensitive measure of photons of energies lower than the average; actually only a lower limit is obtained, since residual cascade effects and neutron background tend to decrease the slope resulting in a lower apparent energy value. Such lower limits of 19 Mev, 14 Mev and 12 Mev were obtained for photons contributing to the (γ,n) reactions on C, Cu and Ag.

The conclusions drawn from the shape of the transition curves of the photons causing (γ,n) reactions thus agree with the results of previous investigators: the energy spread of "effective photons" is small compared to the average energy.

8. Results with zinc detectors. It is believed that the work described so far establishes the validity of the transition curve method of obtaining average energies for the photons responsible for nuclear reactions. The application of this method to several reactions will now be described.

When Zn is bombarded with 330 Mev bremsstrahlung the following activities are observed in large amounts:

(1) 10.1 minutes due to $Zn^{64}(\gamma,np)Cu^{62}$; about 9 percent comes from $Zn^{66}(\gamma,n3p)$ according to part C of this paper.

(2) 38 minutes due to $Zn^{64}(\gamma,n)Zn^{63}$; about 2 percent comes from $Zn^{66}(\gamma,3n)$

as will be seen in part C.

(3) 9.5 hours due to $Zn^{64}(\gamma,2n)Zn^{62}$; less than 1 percent comes from $Zn^{66}(\gamma,4n)$ as shown in part C.

Three other half-lives due to Cu isotopes are produced: these are quite weak for a variety of reasons such as low cross sections, low abundance of starting isotopes, long half-lives or low detecting efficiency. They can be identified in the copper fraction separated from a thick Zn target:

(4) 3.4 hours due to $Zn^{64}(\gamma,p2n)Cu^{61}$; about 22 percent comes from $Zn^{66}(\gamma,p4n)$ as will be seen in part C.

(5) 12.8 hours due to $Zn^{66}(\gamma,pn)Cu^{64}$; about 11 percent comes from other Zn isotopes according to part C.

(6) 63 hours due to $Zn^{68}(\gamma,p)Cu^{67}$; the contributions from Zn^{70} are negligible as shown in part C.

Traces of another activity appeared but due to its relative weakness and short half-life it could not be identified with certainty: it was probably due to the 5 minute Cu^{66}. The Zn metal used was of standard stock: a spectroscopic analysis showed Cu impurities of less than 0.05 percent.

Thus Zn is a particularly suitable element for a comprehensive study: not only can six reactions of five different types be observed and separated, but the decay schemes of the end products are well known and relative yield measurements are possible.

Transition curves for photons responsible for the first three reactions were obtained with 16 mil Zn foils (.03 s.u.) in Geometry 1 and are shown in Figures 11 and 12. The experimental procedures and results will now be discussed:

(1) In order to obtain the relative amount of the 10.1 minute Cu^{62} two samples at a time were bombarded for periods up to 20 minutes, and then

followed on two Eck and Krebs counters for about 150 minutes. This allowed the separation of the short activity from the 38 minute Zn^{63} and traces of longer half-lives. In order that as many points as possible could be obtained on the decay curves, the interchange of samples was only begun after 60 minutes and the resulting counter efficiencies used to obtain the relative activity. From the track length of this transition curve obtained by straight extrapolation beyond 12.5 s.u. an average photon energy of 34 Mev is found.

(2) From the preceding decay curves points for the transition curve for photons effective in producing 38 minutes Zn^{63} are also obtained. Additional points were taken by bombarding Zn foils for up to 1 hour periods, then waiting 60 minutes before starting the comparison counts. The relative activity of two foils then remained constant, indicating that the 10.1 minute Cu^{62} had died out. The track length in this case gives an average photon energy of 21 Mev and the final slope corresponds to 15 Mev.

(3) By bombarding 24 foils in the lead stack for 12 hours and then waiting for 11 hours before starting the measurement of relative activity, the transition curve for the photons producing $Zn^{64}(\gamma,2n)Zn^{62}$ was obtained. The experimental ratios remained constant for as long as the samples could be reliably counted indicating no contributions from much longer activities. The 9.5 hour activity might however be contaminated by the 12.8 hour activity formed by $Zn^{66}(\gamma,np)Cu^{64}$; bombardment of enriched isotopes sets an upper limit 15 percent to this effect which is thus negligible considering the similarity of the curves for the two processes. The resulting transition curve shows a large neutron background: this is not suprising due to the low yield of the reaction $(\gamma,2n)$ (see part C). However this has a small effect on the track length which determines an average photon energy of 32 Mev.

In order to obtain some points on the transition curves of the photons

responsible for the three weak activities a special technique had to be used. The number of product nuclei of a reaction is directly proportional to the target thickness: however due to self-absorption the increase in counting rate is much slower. By dissolving the Zn targets and concentrating the product Cu atoms in a thin sample, the detection efficiency is greatly increased. This was done by adding to a solution in 1N HCl of each Zn detector 1 mg amounts of Cu carrier, precipitating CuS with H_2S, repeating this for complete removal of the Cu activity, and mounting the resulting thin sample on standard cardboard holders under a Scotch tape covering.

The use of standard 9 x 9 inches foils proved impractical due to the large volumes of solution needed; instead each Zn target consisted of three 32 mil disks of 7/8 inch diameter placed behind each other. The lead absorbers were 1 1/2 inch diameter disks. The whole stack was placed at 2 1/3 feet from the synchrotron target in a holder fastened directly on the plastic wall to increase the effective x-ray flux and decrease the beam width. This special set-up has two main disadvantages:

(1) The 0.20 s.u. thickness of the Zn targets is not negligible compared to the absorber thickness; the last sample is behind 7.6 s.u. of Pb and 1.4 s.u. of Zn: since the cascade multiplication effect is smaller in Zn than in Pb taking the effective position of 9.0 s.u. is not quite correct. The difference in size between absorbers and detectors increases this difficulty.

(2) The small size of this geometry makes photon scattering appreciable. In order to correct for these effects a transition curve with polystyrene detectors was taken. These were 32 mils thick and placed between two Cu disks of the same size. The absorber stack at all times consisted of the same lead absorbers and Zn samples except for one C - Cu sandwich monitor

and one detector. The resulting curve was compared with the one taken with the normal Geometry 1: up to 3.5 s.u. no difference was apparent, beyond that the required correction increased rapidly to 56 percent for 9.0 s.u.

Eight Zn samples of the described size were placed into this special set-up and bombarded for 16 hours. The CuS precipitates obtained from the first four samples were placed under four similar end window Victoreen counters connected to automatic Esterline-Angus recorders and followed for 10 days. Frequent interchanges were made to obtain relative counter efficiencies, and a standard was used to keep track of the counter sensitivity. Half-lives of 63 hours, 12.8 hours and 3.4 hours were easily separated from the resulting decay curves. The activities of the four remaining CuS samples were compared to the others after all but the 63 hour half-lives had died out. Thus the points plotted in Figures 11 and 12 were obtained after application of the corrections for geometry as explained above.

The three points of the transition curve for the photons causing $Zn^{66}(\gamma,np)Cu^{64}$ should be close to the other (γ,np) curve; the average 5 percent deviation gives an estimate of the accuracy of this particular work. The transition curve for the photons responsible for $Zn^{68}(\gamma,p)Cu^{67}$ is the most interesting: by extending it beyond 9 s.u. by analogy with the other curves the track length gives an average photon energy of 27 Mev. Only three points are available for the x-rays causing $Zn^{64}(\gamma,p2n)Cu^{61}$: they indicate an average energy of around 60 Mev.

The detailed shape of the (γ,p) curve is of particular interest as will be discussed later; indications exist that in this case the energy range of "effective photons" is wider for the (γ,n) process. It is unfortunate that the poor accuracy attained in this case makes impossible any discussion along this line.

9. Results with tantalum detectors.

Irradiation of tantalum metal with the synchrotron beam results in the production of several activities:

(1) A half-life of the order of 5 minutes too weak and short-lived for investigation with the present procedure.

(2) A half-life of 70 minutes not previously reported in this region of the peridoic table and chemically identified as a rare earth.* The reaction resulting in the formation of this new activity thus proceeds with the emission of at least two protons.

(3) A half-life of 8 hours due to $Ta^{181}(\gamma,n)Ta^{180}$.

(4) Several half-lives of the order of days that could not be separated.

The transition curve for photons responsible for the (γ,n) reaction is shown in Figure 13: it was obtained by putting 24 foils of 6 mil Ta sheet (.043 s.u.) into the lead stack of Geometry 1, bombarding for 12 hours and then waiting an equal period before starting the measurement of relative activity. The activity ratios however did not remain constant, the maximum decreased slowly indicating that one or more activities of longer half-life had been produced by higher energy photons. The given curve was taken at about the time where the largest maximum was observed: a comparison of its shape with that of the transition curve for $Cu^{63}(\gamma,n)Cu^{62}$ is of interest. For lead thicknesses of less than 5.5 s.u. the Cu curve is above the one for Ta; the reverse is true beyond 5.5. s.u. This effect is of course due to the long half-lives produced by high energy photons that could not be separated; the same shape however would also be obtained if more high energy photons participated in the (γ,n) reaction in Ta than in Cu. The monitor foil contained

---

*I am indebted to Dr. J. Wilkinson for carrying out the chemical separations in this case.

about 10 percent of these long half-lives.

Due to this difficulty the average photon energy of 21 Mev as obtained from the track length is not very reliable and its deviation from 16 Mev where the peak of the cross section occurs[10] is not very suprising.

A few points of the transition curve for the photons causing the new rare earth activity were taken with 21 mil (.15 s.u.) Ta disks placed in Geometry 2. The induced activity was followed for 24 hours and the 8 hour Ta^{180} subtracted. The results are shown in Figure 13: by extrapolating the straight line to larger thicknesses an average photon energy of 70 Mev is found from the track length.

10. Results with bismuth detectors. The bombardment of Bi^{209} with the 330 Mev synchrotron beam leads to many activities with half-lives ranging from minutes to days. The closest known short half-lives that could have been produced ar Tl^{207}(5 min.), Tl^{206}(4 min.), Bi^{204}(12 hrs.) and Pb^{203} (52 hrs.). Other activities present masked any of these known ones, and no definite half-lives could be obtained from analysis of the decay curves.

To obtain some information on the energy of the photons responsible, a transition curve was taken with the standard Geometry 1: the Bi detectors however were in the form of 2 7/16 inch diameter disks of 30 mils thickness (.14 s.u.).* After a 3 1/2 hour bombardment the activities of the samples were compared with end window Victoreen counters and the results are shown in Figure 14 which also has a plot of the transition curve for the photons causing $Zn^{64}(\gamma,2n)Zn^{66}$ for comparison. Assuming a straight line absorption curve going through these points, an average photon energy of 90 Mev is obtained. The absorption coefficient obtained from this line corresponds to

---

*I am indebted to E. Kelly for these disks which he cast in vacuum from Bi bricks listed as 99.8 percent pure.

an energy lower than 90 Mev indicating that multiplication of the "effective photons" is still important.

This steep transition curve represents results taken during the first two hours after the end of the bombardment; after that it started to rise slowly indicating that the longer half-lives were due to lower energy photons. The low activity of the samples when the effect became appreciable precluded quantitative observations. Further work, especially chemical separations, is needed.

11. Results with lead detectors. When Pb is irradiated in the synchrotron beam many activities appear besides the expected Tl^{206}(4 min.) and Tl^{207}(5 min.). The other shorter half-lives in this region are: Hg^{205}(5.5 min.), $Pb^{205,203}$(10 min.), Pb^{203}(52 hours), Pb^{201}(8 hours). The observed decay curve could not be resolved into these activities due to the apparent presence of other half-lives.

18 mil thick Pb absorbers (.09 s.u.) were used in the standard Geometry 1 to determine a transition curve for the "effective photons." The results as shown in Figure 13 are quite similar to the case of Bi. The relative activity measurements were started one hour after the end of the bombardment to allow for the decay of the 4 and 5 minutes Tl activities and the same transition curve observed over a period of eight hours. After that time it began to rise slowly and the curve for the long half-lives shown in Figure 13 was taken 36 hours after the end of the bombardment. Approximate values of 90 Mev and 70 Mev are obtained for the quantum energies responsible for the two curves respectively. The shape at large depths of the short half-life curve indicates an appreciable neutron background. Further work is indicated.

12. Conclusion. The work presented illustrates several possible applications of the transition curves of "effective photons" responsible for nuclear

reactions:

(1) In the case where one activity only is present in appreciable amounts (such as γ,n on C, Cu, Zn, Ag; γ,2n on Zn) many experimental points can be obtained and the curves are accurately determined. It is estimated that the track length can then be measured with a 3 percent accuracy. The accuracy of the expression (2) is estimated by Eyges to be 10 percent around 20 Mev, 5 percent at 30 Mev and higher. Thus the average "effective photon" energy is obtained within 10 percent around 20 Mev and 6 percent at 30 Mev and higher energies. The relative value of the energies should be accurate to within 5 percent.

(2) When the activity under investigation has to be obtained from analysis of decay curves, the expected error depends on the ease of such analysis and the number of points obtained. For example it is believed that the $Zn^{64}(\gamma,np)Cu^{62}$ average energy is good to 10 percent and the $Ta^{181}(\gamma,2p..)$R.E. value to 20 percent.

(3) Where accurate curves are obtainable eventual contributions from high energy photons should be detectable at small absorber thickness, from low energy photons at large absorber thickness.

(4) When new activities or reactions are found (Ta, Pb, Bi) a few points give an estimate of the photon energy responsible, information valuable in determining the processes responsible.

(5) A check on the accuracy of the approximations used in shower theory is possible in certain cases where discrepancies occur that cannot be due to eventual contributions of high or low energy photons (detailed shape of the (γ,n) curve of Cu).

The main advantages of the transition curve method of finding average "effective photon" energies are:

(1) The maximum beam energy need not be varied which in the case of the Berkeley synchrotron would be very time consuming.

(2) No beam monitor whose energy dependence has to be accurately known is required.

(3) For long half-lives only one bombardment is needed to obtain the average energy: since our bombardment times are of the order of the half-life this is important.

The main disadvantage comes from the absence of detailed information on the shape of the excitation functions.

C. REACTION CROSS SECTIONS AND RELATIVE YIELDS

1. Introduction. When a thin target is bombarded with a monoenergetic beam of particles or photons the reaction cross section σ is defined by:

$$n = N\sigma q \tag{4}$$

where n = number of reactions per unit time of bombardment

N = number of target nuclei per unit area

q = number of incident particles per unit time

This definition is not immediately applicable to the case of a target placed in the synchrotron beam: photons of all energies are present in the beam and their spectral distribution is proportional to expression (1). For a small energy interval one can still write:

$$dn = N\,\sigma(W)\,dq(W) \tag{5}$$

where $dq(W)$ = number of photons incident per unit time of energy between W and $W + dW$

$\sigma(W)$ = value of the reaction cross section at the energy W

dn = number of reactions per unit time produced by the photons $dq(W)$

How can $dq(W)$ be obtained? Blocker, Kenney and Panofsky[22] have developed a method by which the energy incident on the target per unit time can be measured: their results are given in terms of a quantity Q which is defined by

$$I = Q\,W_o \tag{6}$$

where $I = \int_0^{W_o} W\,dq(W)$ = total energy incident per unit time on the target

W_o = maximum beam energy

The theoretical energy distribution of the photons in the beam is given by expression (1). Figure 15 shows a plot of a function $f(W)$ proportional to $Wdq(W)$ versus W as calculated from (1) for the Berkeley synchrotron: the area under the curve is proportional to I. This function $f(W)$ is defined

as follows:

$$dq(W) = k \frac{f(W)}{W} dW \tag{7}$$

where k is a proportionality constant such that f(W) has the numerical value given by the ordinate of Figure 15. The constant k is immediately determined by numerical integration under the graph of f(W) since:

$$I = QW_o = \int_o^{W_o} W dq(W) = k \int_o^{330} f(W) dW = 51.3\ k\ \text{Mev}$$

so that:

$$dq(W) = \frac{Q}{51.3} \frac{W_o}{W} f(W)\ dW \tag{8}$$

Equation (5) can now be written:

$$dn = N \frac{Q}{51.3} W_o\, \sigma(W) \frac{f(W)}{W} dW \tag{9}$$

and the total number of reactions per unit time is given by:

$$n = N \frac{Q}{51.3} W_o \int_o^{W_o} \sigma(W) \frac{f(W)}{W} dW \tag{10}$$

The work reported in this paper gives no detailed information about the shape of $\sigma(W)$: as was indicated in section 7 of part B there is good evidence that for the majority of reactions the cross section has only an appreciable value near the mean energy W_{av}. It will be assumed that:

$$W_{max} = W_{av} + \frac{1}{2}\Delta W \qquad W_{min} = W_{av} - \frac{1}{2}\Delta W \quad \text{where} \quad \Delta W < W \tag{11}$$

Equation (5) can then be written:

$$n = N \frac{Q}{51.3} W_o \int_{W_{av}-\frac{1}{2}\Delta W}^{W_{av}+\frac{1}{2}\Delta W} \sigma(W) \frac{f(W)}{W} dW \tag{12}$$

As can be seen from Figure 15 f(W) is a very slowly varying function of W

up to 300 Mev so that by keeping only the first term in its Taylor expansion the factor $f(W_{av})$ can be taken out of the integral sign. The term $\frac{1}{W}$ can also be replaced by $\frac{1}{W_{av}}$ outside of the integral sign: this neglects terms of the order $\left(\frac{\Delta W}{W}\right)^2$ if $\sigma(W)$ is symmetrical around W_{av}. The final result is then:

$$n = N \frac{Q}{51.3} \frac{W_o}{W_{av}} f(W_{av}) \bar{\sigma} \qquad (13)$$

where the integrated cross section $\bar{\sigma} = \int_{W_{av}-\frac{1}{2}\Delta W}^{W_{av}+\frac{1}{2}\Delta W} \sigma(W)\, dW \qquad (14)$

In cases where W_{av} is not known, or where approximation (11) is not applicable, the integrated cross section cannot be obtained. In that case a reaction yield y can be defined by:

$$n = N Q y \qquad (15)$$

where the other symbols have the same meaning as above. This yield y then corresponds to a cross section obtained by assuming that all photons in the beam are effective, and that the number of incident quanta is given by $\frac{I}{E_o}$.

In practice the relative number of two reactions 1 and 2 is often measured at the same time: the relative yields are then given by:

$$\frac{y_1}{y_2} = \frac{n_1}{n_2} \frac{N_2}{N_1} \qquad (16)$$

and the relative cross sections by

$$\frac{\bar{\sigma}_1}{\bar{\sigma}_2} = \frac{(W_{av})_1}{(W_{av})_2} \frac{f(W_{av})_2}{f(W_{av})_2} \frac{n_1}{n_2} \frac{N_2}{N_1} \qquad (17)$$

It is seen that the average "effective photon" energy has to be known to obtain absolute or relative cross sections: the transition curve method is especially suitable for this.

2. Relative yield measurements. The reactions under investigation are identified by the radioactivity of the product nuclei. The measured or extrapolated activity at the end of the bombardment is proportional to the number of reactions after several factors have been taken into account:

(1) The counters used for this work are standard Victoreen counters with a 3 mg/cm^2 end window: they are primarily sensitive to β-particles. The number of disintegrations corresponding to the number of observed counts can be calculated if the decay scheme is known.

(2) Self-absorption of β-particles reduces the apparent yield. This effect can be minimized by the use of very thin samples, targets of equal thickness if the β-spectra of the two activities are the same, or by preparing a thin sample from the target by chemical separation. Where none of these alternatives can be used, a self-absorption curve has to be taken with samples of varying thickness.

(3) Since the half-lives of the product nuclei are in general different, the decay of these nuclei and the variation in beam intensity during the bombardment must be taken into account unless the time of irradiation is much shorter than the half-lives. The following well-known expression is used:

$$A = n\int_0^T \theta(t)\, e^{-\lambda t}\, dt \qquad (18)$$

where A = number of product nuclei at the end of the bombardment

n = number of reactions per unit time of bombardment

T = duration of bombardment

$\theta(t)$ = function directly proportional to the number of photons hitting the target between t and $t + dt$ and normalized such that

$$\int_0^T \theta(t)\, dt = 1$$

λ= decay constant of radioactive product

The beam is monitored with an ionization chamber. By taking readings at regular time intervals short compared to $1/\lambda$ on an integrator connected to the monitor chamber, $\theta(t)$ is determined and the integral in equation (18) can be evaluated numerically. This procedure was followed where required.

When the relative yield of two reactions is being measured by bombardment of two samples, foils or powder targets of identical area are placed behind each other in the beam. In this way the same number of photons pass through both targets and the counter geometry can be made identical.

The primary purpose of the yield measurements was to obtain information for several reactions from the same element: Zn was chosen since not only were such measurements relatively convenient, but several transition curves could also be obtained in this case. The results are summarized in Table III: where W_{av} is known, the relative cross section was calculated using equation (17). All values were normalized to the reaction $Cu^{63}(\gamma,n)Cu^{62}$ since the Cu^{62} activity provided a convenient reference in most measurements. Except where noted otherwise the yield values represent the average of two or more measurements. Table III also lists the decay schemes of the product nuclei.

Experimental procedures will now be summarized for each case:

(1) $C^{12}(\gamma,n)C^{11}$ 20 minutes. One 5 mil polystyrene and one 1/3 mil Cu disks were bombarded together and the resulting activities compared. Self-absorption was neglected.

(2) $Cu^{65}(\gamma,n)Cu^{64}$ 12.8 hours. One 1/3 mil Cu foil was bombarded for 8 hours and then followed for 5 days. The resulting decay curve yielded 10 minute, 2.6 hour and 12.8 hour half-lives from which the quoted result was obtained. The intermediate half-life, probably due to Cu^{61} and Co^{61} could not be used. Self-absorption was neglected.

(3) $Zn^{64}(\gamma,n)Zn^{63}$ 38 minutes and $Zn^{64}(\gamma,np)Cu^{62}$ 10 minutes. Cu and Zn disks, both 1/3 and 1 mil thick were irradiated together; the decay was then followed with two counters whose relative efficiency had been measured with irradiated Cu foils. The resultant yield value of the (γ,np) reaction was reduced by 9 percent to take contamination from $Zn^{66}(\gamma,3np)$ into account. No corrections for self-absorption seemed necessary.

(4) $Zn^{64}(\gamma,2n)Zn^{62}$ 9.5 hours. The low yield of this reaction made the use of a thick target necessary and to prevent contamination by the 12.8 hour product of $Zn^{66}(\gamma,np)Cu^{64}$ enriched $Zn^{64}O$ was used. By comparing the amount of the 10 minute activity from Cu^{62} to the amount of 9.5 hour activity from Zn^{62} (which decays nearly entirely by K capture to Cu^{62}) self-absorption need not be considered. Actually Zn^{63} obtained in 20 minute and 10 hour bombardments was used as an intermediate reference.

(5) $Zn^{68}(\gamma,p)Cu^{67}$ 63 hours; $Zn^{66}(\gamma,pn)Cu^{64}$ 12.8 hours and $Zn^{64}(\gamma,p2n)Cu^{61}$. To obtain large enough a counting rate for accurate observation and to prevent contamination from Zn activities, Cu was separated with H_2S from 13 gr of $ZnSO_4 \cdot 7H_2O$ irradiated for 12 hours in the synchrotron beam. This separation could be carried out in a time short enough so that the CuS sample was placed under the counter 15 minutes after the end of the bombardment: this allowed the use of the product of $Zn^{64}(\gamma,pn)Cu^{62}$ as reference activity. Since only 2 mg of Cu carrier were added and the CuS placed on a thin filter paper, self-absorption was neglected. Reduction of the observed yield of Cu^{64} by 11 percent and of Cu^{61} by 22 percent was made to take into account the production of these activities from higher Zn isotopes.

(6) $Zn^{66}(\gamma,3n)Zn^{63}$ 38 minutes, $Zn^{66}(\gamma,p3n)Cu^{62}$ 10 minutes and $Zn^{66}(\gamma,p4n)$ 3.4 hours. The yield of these reactions relative to reactions from Zn^{64} leading to the same product nuclei was obtained by simultaneous bombardment

of equal amounts of enriched $Zn^{64}O$ and $Zn^{66}O$. The decay was followed with two counters whose relative efficiency was determined by sample interchanges. From the known composition of the samples the yields can be computed; from the given uncertainties in the isotopic analysis alone the result of the $(\gamma,3n)$ reaction could be off by a factor of two, while for $(\gamma,3np)$ the result is undetermined by 15 percent. That the observed activities are not completely due to the Zn^{64} present in both compounds is shown by the different activity ratios of the 10 minute, 38 minute, 3.4 hour half-lives in the two samples.

(7) $Zn^{67}(\gamma,4n)Zn^{63}$ 38 minutes. Simultaneous bombardment of $Zn^{64}O$ and $Zn^{67}O$ in equal amounts leads to no observable effect due to this reaction; the quoted upper limit is estimated from detectable activity differences and uncertainties in the isotopic constitution.

The yields of the reactions due to high energy photons in Ta, Pb and Bi could not be measured due to the lack of information on the decay schemes of the product nuclei. No yield data is being presented for reactions proceeding with the emission of more than one proton: Friedlander and Perlman[7] give the yield of Co^{61} from Cu as less than 1 percent of the (γ,n) yield, showing such reactions to be rare. This particular result is being checked at the present time.

3. Integrated cross section of the reaction $Cu^{63}(\gamma,n)Cu^{62}$. The reaction $Cu^{63}(\gamma,n)Cu^{62}$ was chosen for a cross section measurement because of its large yield, energetic β-spectrum and freedom from contamination of the product activity in the case of short bombardments. The reaction $Cu^{66}(\gamma,3n)Cu^{62}$ contributes less than 2 percent to the observed activity which can be neglected. From the transition curve of the x-rays responsible for this reaction the average "effective photon" energy is known to be 20 Mev so that the integrated cross section $\bar{\sigma}$ can be obtained using equation (13) after n

and Q have been determined.

The energy of the beam passing through a selected area has to be known. The method used for this measurement was developed by Blocker, Kenney and Panofsky and is described in detail elsewhere.[22] Thus the procedure used for the determination of the cross section will only be outlined. The set-up used consists of the standard monitor chamber, a two inch collimator and a large ionization chamber of known geometry placed in the beam respectively at 4 ft., 4 3/4 ft. and 5 3/4 ft. from the synchrotron Pt target. A thin polystyrene sample holder was situated on the front foil of the large chamber so that 7/8 inch diameter disks could be irradiated under repeatable geometrical conditions.

First the monitor chamber was calibrated against the beam energy passing through the selected target area.* Pb, Cu and Al disks of 7/8 inch diameter and a thickness such as to contain the same number of electrons were placed into the sample holder, irradiated consecutively with a certain amount of beam as integrated by the monitor chamber, and the resulting ionization in the large chamber measured. Background run readings were frequently obtained. Taking Pb-Al and Pb-Cu differences for the ionization due to pairs eliminates both Compton electrons and general background. From the average of these two differences the energy passing through the target area per unit integrated beam can be calculated (see reference (22)) using the known pair production cross section.

Cu disks of 7/8 inch diameter and 12 mils thick were then placed in the sample holder and irradiated with about the same beam intensity as was used for the monitor chamber calibration. From the integrated beam as obtained

---

*I am much indebted to W. Blocker and R. Kenney for this calibration.

from the monitor chamber the total energy having passed through the Cu disk was calculated and Q obtained from the irradiation time and equation (6).

The activity of the sample at the end of the bombardment was calculated from the total number of counts obtained in 4 or 8 minute periods by assuming a 10.1 minute half-life. The corresponding number of radioactive nuclei A in the Cu disk was obtained by comparison with an absolute β standard belonging to Professor McMillan.* The size of the active U_3O_8 deposit on this standard determined the diameter of the sample disks, and the counting was done on shelf 2 (1 inch from the counter window) to further minimize geometrical effects. The bombardments were either of 2 minute duration or longer, depending on the amount of time the beam remained of constant intensity. With the help of equations (18) and (13) the integrated cross section was finally obtained.

This method was used in two runs spaced 4 months apart. The first time $\bar{\sigma}$ = 1.03 Mev-barns was obtained from two Cu samples that agreed within 4 percent. The second time $\bar{\sigma}$ = 0.92 Mev-barns was found with three Cu samples that agreed within 8 percent. The average of these two determinations gives a preliminary value of

$$\bar{\sigma} = 1.0 \text{ Mev-barns}$$

which still has to be corrected for self-absorption and scattering in the sample. This is estimated to change the answer by less than 15 percent.

Lawson and Perlman[8] using their pair spectrometer to measure the number of photons in a 15 Mev interval centered at 30 Mev obtain for the cross section of the reaction $C^{12}(\gamma,n)C^{11}$ a value of $\bar{\sigma}$ = 0.148 Mev-barns.

---

*This standard was recently calibrated by L. Aamodt using as standards Na^{24} (β-γ coincidences), Au^{198} (β-γ coincidences), RaD,E,F (α-particles). These three calibrations checked within 5 percent.

They also quote $\bar{\sigma}$ = 1.5 Mev-barns for the reaction $Cu^{63}(\gamma,n)Cu^{62}$: this was apparently calculated using the 1:14 measured relative yield, cross section peaks at 30 Mev and 22 Mev and a 1/E bremsstrahlung spectrum. To compare this cross section with out measurement the "effective photon" energy should be taken at 20 Mev and the actual shape of the photon spectrum used. Assuming the later to be similar to the one shown in Figure 15 (with abscissa values divided by 3.3) a value of $\bar{\sigma}$ = 1.24 Mev-barns is obtained for $Cu^{63}(\gamma,n)Cu^{62}$. The agreement appears satisfactory.

D. DISCUSSION

1. Summary of results. A method using the transition curves in Pb of those x-rays responsible for a nuclear reaction has been applied to obtain the average "effective photon" energy W_{av} in several cases. By combining these values of W_{av} with measured relative yields, relative cross sections were calculated; the main target element used in this investigation was zinc.

The total integrated cross section for photon absorption by one nucleus is of interest: this can be estimated in the case of Zn by using $\overline{\sigma}$ = 1 Mev-barns for $Cu^{63}(\gamma,n)Cu^{62}$. Adding the integrated cross sections for the (γ,n), $(\gamma,2n)$, (γ,p), (γ,pn), $(\gamma,p2n)$ reactions on Zn 1.6 Mev-barns is obtained. The relative yields but not W_{av} is known for the $(\gamma,3n)$, $(\gamma,p3n)$ and $(\gamma,p4n)$ processes; by estimating W_{av} from the nuclear binding energy these reactions should contribute about 0.2 Mev-barns. We obtain thus

$$\overline{\sigma}_{total} \geqslant 1.8 \text{ Mev-barns}$$

for a lower limit of the total integrated photon absorption cross section on Zn. It seems probable that the reactions that were not observed would add no large contributions to this value. The fact that not all of the observed reactions started from the same Zn isotope should not affect this result greatly.

In a similar manner a lower limit for the average photon energy $\overline{W}$ absorbed by the Zn nucleus can be estimated using $\overline{W} = \frac{\sum \sigma W_{av}}{\sum \sigma}$: the result is

$$\overline{W} = 30 \text{ Mev}$$

2. Comparison with other experiments. As was pointed out in part B of this paper the average "effective photon" energy as obtained from transition curves checks the two cases where values by another method are available. The integrated cross section for $Cu^{63}(\gamma,n)$ is in agreement with the

measurement of Lawson and Perlman[8] within the estimated errors.

Perlman and Friedlander[7] have measured the relative yield of some reactions of the same type as were obtained from Zn by using Cu and Ge. In particular $(\gamma,2n)$, (γ,p) and (γ,pn) yields are given by these authors, and although the individual agreement with similar values for Zn only check within a factor of three, the sum of the yields of these reactions are the same. The relatively large yield of the (γ,pn) reactions might be suprising; Gaerttner and Yeater[23] have measured the cross sections for such a reaction on O_2 and N_2 and find 0.30 Mev-barn in this case, of the same magnitude as our result for the same reaction on Zn.

It is of interest to consider the decay of the compound nucleus Zn^{64} when excited by different methods. Ghoshal[24] has obtained this compound nucleus by α-particle bombardment of Ni and proton bombardment of Cu, while in this paper the excitation with x-rays has been described. The cross section for formation of the compound nucleus depends of course on the method of excitation, only the decay might be independent of this factor if the nucleus has lost all "memory" of its origin. This means that the role of competing reactions at a given excitation energy might be the same independently of the means of formation of the compound nucleus. Ghoshal finds for the incident α-particle energy at the peak of the (α,n) reaction 20 Mev, at the peaks of the $(\alpha,2n)$ and (α,pn) processes 31 Mev; the excitation curves for the two methods of compound nucleus formation are very similar. Since α-particles contribute little binding energy to the compound nucleus, it is not suprising to find W_{av} for (γ,n) at 21 Mev, for $(\gamma,2n)$ at 32 Mev and for (γ,pn) at 34 Mev. In addition Ghoshal finds that the relative yield of $(\alpha$ or $p,pn)$ is four times larger than the yield of $(\alpha$ or $p,2n)$; we found six for this ratio which is quite similar considering that we are comparing peak and integrated

cross sections. There appears to be no evidence from these facts at least that the decay of the compound nucleus depends on the method of formation.

Levinthal and Silverman[25] have obtained energy and angular distributions of protons emitted by several elements irradiated in the synchrotron beam. They find a relatively large number of high energy protons that would not be expected according to the statistical theory, and these protons show an asymmetrical angular distribution. They conclude from these facts that photons of an energy of about 30 Mev and higher produce part of the time a direct photoelectric effect. This means that the (γ,p) reaction is not necessarily produced by photons grouped in a narrow region around the average energy, and this should be noticeable in the shape of the corresponding transition curve. It is unfortunate as was pointed out before that the accuracy obtained for this case does not warrant any conclusions along this line.

3. Comparison with proposed models for nuclear photon absorption. Following the work of Bothe and Gentner the theory of the nuclear photoeffect on heavy nuclei became of interest and calculations were carried out by Weisskopf[26] and others assuming quadrupole transitions only. The main reason for this assumption was based on the experimental fact that the γ-rays emitted by excited nuclei were mainly of a quadrupole character due to the large mutual binding of the nucleons. The results of these theoretical investigations were unable to explain the large integrated cross section and the rapid rise of the excitation curve beyond 17 Mev of the reaction $Cu^{63}(\gamma,n)Cu^{62}$ as found by the G. E. group.

Goldhaber and Teller[27] then suggested the existence of dipole transitions at a nuclear excitation energy of about 20 Mev where correlation among nucleon should become small. These two authors used a specific model in which all protons move together against all neutrons: this leads to a very

sharp resonance absorption and scattering of photons by Cu around 20 Mev. The small yield of the $(\gamma,2n)$ compared to the (γ,n) reaction would then be explained by the closeness of the absorption energy to the $(\gamma,2n)$ threshold. The work reported in this paper on the photonuclear reactions from Zn does not appear to support these views for this case: although the (γ,n) reaction has the largest yield, the other reactions contribute about an equal amount to the total absorption; in addition, the average photon energies responsible for the higher order reactions are larger than the energy causing (γ,n). It has been suggested[28] that a second resonance peak around 40 Mev might contribute to the photon absorption, but the small magnitude of the $(\gamma,3n)$ yield does not support this view.

In a recent paper Levinger and Bethe[29] have used sum rules to calculate the total integrated absorption cross section $\overline{\sigma}_{total}$ and the mean energy for photon absorption $\overline{W}$ for both dipole and quadrupole transition. They conclude from quite general considerations that the calculated quadrupole capture probability is much too small, and that dipole transitions give the correct order of magnitude if exchange forces are included. No special model for the absorption is assumed, only rectangular or Yukawa wells are taken for the n-p force. The two authors obtain detailed expressions for $\overline{W}$ and $\overline{\sigma}_{total}$ as a function of the parameter x, the fraction of the n-p force being due to exchange forces. For $\overline{W} = 30 \pm 3$ Mev one obtains for the Yukawa well with $r_o = 1.50 \times 10^{-13}$ cm, $x = 0.53 \pm 0.09$ and with $r_o = 1.37 \times 10^{-13}$ cm, $x = 0.36 \pm 0.09$. Taking for the integrated absorption cross section $\overline{\sigma}_{total} = 1.8 \times 0.5$ Mev-barns one obtains $x = 1.2 \pm 0.7$. From the Berkeley n-p scattering experiments a value of $x = 0.55 \pm 0.05$ has been obtained. The agreement is not bad.

Acknowledgments. It is a pleasure to thank Professor A. C. Helmholz under whose direction this work was carried out for many helpful suggestions and assistance, and Professor E. McMillan for his constructive interest and support. Several conversations with Professor R. Serber on the interpretation of the transition curves proved very valuable. The author is very much indebted to Dr. L. Eyges for applying the shower theory to this problem and performing the required calculations. Mr. J. Rose assisted in some of the measurements and his help is much appreciated. Finally this work would not have been possible without the fine cooperation of Mr. W. Gibbins and the synchrotron crew.

This work was sponsored by the U. S. Atomic Energy Commission.

TABLE I

Experimental and theoretical track length ratios

for 330 Mev and 200 Mev bremsstrahlung

Reaction	Beam Energy	Observed Track Length	Ratio Exp.	Ratio Theor.
$C^{12}(\gamma,n)C^{11}$	330 Mev	7.1	1.42	1.50
	210 ± 5 Mev	5.0		
$Cu^{63}(\gamma,n)Cu^{62}$	330 Mev	11.1	1.51	1.55
	206 ± 5 Mev	7.4		

TABLE II

Relative yield of some reactions induced by

50 Mev, 100 Mev and 330 Mev bremsstrahlung

Reaction	50 Mev[a]	100 Mev[a]	330 Mev
$C^{12}(\gamma,n)C^{11}$	.066	.070	.072
$Cu^{63}(\gamma,n)Cu^{62}$	1.0	1.0	1.0
$Cu^{65}(\gamma,n)Cu^{63}$	.97	1.2	1.2
$Zn^{64}(\gamma,n)Zn^{63}$	.79	.75	0.83

(a) Values taken from Perlman and Friedlander[7]

TABLE III

Average "effective photon" energy W_{av}, relative yields and integrated cross sections $\bar{\sigma}$ for some nuclear reactions induced by 330 Mev bremsstrahlung

Reaction	Product half-life[a]	Product betas and energy (Mev)[a]	Track length (shower units)	W_{av} (Mev)	y_{rel}	$\bar{\sigma}_{rel}$
$C^{12}(\gamma,n)C^{11}$	20 min.	β^+ 0.99	7.1	30	0.072	0.11
$Cu^{63}(\gamma,n)Cu^{62}$	10 min.	β^+ 2.92[c]	11.1	20	1.0	1.0
$Cu^{65}(\gamma,n)Cu^{64}$	12.8 hrs.	β^+ 0.64(15%); β^- 0.57(31%) K (54%)		21[d]	1.2	1.3
$Zn^{64}(\gamma,n)Zn^{63}$	38 min.	β^+ 0.47(1%); 1.40(7%); 2.36(85%) K (7%)	10.3	21	0.83	0.87
$Zn^{68}(\gamma,p)Cu^{67}$	63 hrs.[b]	β^- 0.56	8.0[d]	27[d]	0.12[e]	0.16
$Zn^{64}(\gamma,2n)Zn^{62}$	9.5 hrs.	β^+ 0.66(9.5%)[c] K (90.5%)	6.5	32	0.039	0.065
$Zn^{64}(\gamma,pn)Cu^{62}$	10 min.	see above	6.1	34	0.21	0.38
$Zn^{66}(\gamma,pn)Cu^{64}$	12.8 hrs.	see above		34[d]	0.14[e]	0.25
$Zn^{66}(\gamma,3n)Zn^{63}$	38 min.	see above			0.029	
$Zn^{64}(\gamma,p2n)Cu^{61}$	3.4 hrs.	β^+ 1.20	3.2[d]	65[d]	0.029[e]	.10
$Zn^{67}(\gamma,4n)Zn^{63}$	38 min.	see above			<.02	
$Zn^{66}(\gamma,p3n)Cu^{62}$	10 min.	see above			0.033	
$Zn^{66}(\gamma,p4n)Cu^{61}$	3.4 hrs.	see above			0.014	
$Ag^{107}(\gamma,n)Ag^{106}$	24 min.	β^+ 2.0 Mev	12.1	18		
$Ta^{181}(\gamma,2p...$ Rare Earth	70 min.[b]	?	2.9	70		
$Pb(\gamma,?)$	hours[b]	?	2.3	90		
$Pb(\gamma,?)$	days[b]	?	3.0	70		
$Bi(\gamma,?)$	hours[b]	?	2.3	90		

(a) Unless otherwise stated values taken from G. T. Seaborg and I. Perlman, Rev. Mod. Phys. 20, 585 (1948)
(b) Half-life observed in this work.
(c) R. W. Hayward, private communication.
(d) Only a few points were obtained for the transition curve, and the energy W_{av} estimated by comparison with complete curves.
(e) One experiment only.

BIBLIOGRAPHY

(1) J. Chadwick and M. Golhaber, Nature 134, 237 (1934)

(2) L. Szilard and T. A. Chalmers, Nature 134, 494 (1934)

(3) W. Bothe and W. Gentner, Z. Phys. 106, 236 (1937)

(4) W. Bothe and W. Gentner, Z. Phys. 112, 45 (1937)

(5) O. Huber, O. Lienhard, P. Scherrer and H. Waeffler, Helv. Phys. Acta 16, 33, 228, 431 (1943); 17, 139, 195, 251 (1944)

(6) O. Hirzel and H. Waeffler, Helv. Phys. Acta 19, 214 (1946); 20, 373 (1947); 21, 200 (1948)

(7) M. L. Perlman and G. Friedlander, Phys. Rev. 74, 442 (1948)
M. L. Perlman, Phys. Rev. 75, 989 (1949)

(8) J. L. Lawson and M. L. Perlman, Phys. Rev. 74, 1190 (1948)

(9) G. C. Baldwin and G. S. Klaiber, Phys. Rev. 70, 259 (1946); 71, 3 (1947); 73, 1156 (1948)

(10) J. McElhinney, A. O. Hanson, R. A. Becker, R. F. Duffield and B. C. Diven, Phys. Rev. 75, 542 (1949)

(11) G. A. Price and D. W. Kerst, Phys. Rev. 77, 806 (1950)

(12) B. Rossi and K. Greissen, Rev. Mod. Phys. 13, 240 (1941)

(13) W. Heitler, The Quantum Theory of Radiation, Oxford University Press, 1944

(14) J. Rober and L. W. Nordheim, Phys. Rev. 75, 444 (1949)

(15) J. S. Laughlin, L. S. Skaggs, A. O. Hanson and J. J. Orlin, Phys. Rev. 73, 1223 (1948)

(16) J. F. Carlson and J. R. Oppenheimer, Phys. Rev. 51, 220 (1937)

(17) H. J. Bhabha and W. Heitler, Proc. Roy. Soc. 159, 432 (1937)

(18) L. Eyges, provate communication

(19) R. L. Walker, Phys. Rev. 76, 527 (1949)

(20) J. L. Lawson, Phys. Rev. 75, 433 (1949)

(21) R. Serber, private communication

(22) W. Blocker, R. Kenney and W. Panofsky, UCRL-565

(23) E. R. Gaerttner and M. L. Yeater, Phys. Rev. 77, 714 (1950)

(24) S. Ghoshal, private communication

(25) C. Levinthal and A. Silverman, private communication

(26) W. F. Weisskopf, Phys. Rev. 59, 318 (1941)

(27) M. Goldhaber and E. Teller, Phys. Rev. 74, 1046 (1948)

(28) M. Goldhaber, private communication

(29) J. S. Levinger and H. A. Bethe, Phys. Rev. 78, 115 (1950)

FIGURE CAPTIONS

Figure 1 Position of absorber stack with respect to the synchrotron and different geometries used in the experiment.

Figure 2 Transition curves in Pb of x-rays causing (γ,n) reactions on C, Cu and Ag.

Figure 3 Transition curves in Pb of x-rays causing (γ,n) reactions on C, Cu and Ag on semi-logarithmic plot.

Figure 4 Beginning of transition curves in Pb of x-rays causing (γ,n) reactions on C and Cu. Theoretical curves for 20 Mev and 30 Mev photons are given on the respective plots.

Figure 5 Synchrotron beam width at 5 1/3 feet from the Pt target taken in front and behind 2.7 s.u. of Pb using Cu detectors. The lower curve shows the sensitivity of an Eck and Krebs counter.

Figure 6 Points for the transition curve in Pb of x-rays causing $C^{11}(\gamma,n)C^{11}$ as obtained with Geometry 1 and Geometry 2. The theoretical curve for 30 Mev photons is also shown.

Figure 7 Influence of geometry on transition curve in Pb of x-rays causing $Cu^{63}(\gamma,n)Cu^{62}$. The theoretical curve for 20 Mev photons is shown by the dotted curve.

Figure 8 Top plot: influence of backscattering on the transition curve of x-rays responsible for $Cu^{63}(\gamma,n)Cu^{62}$. The ordinate represents the ratio of the observed activity with no lead backing y_o to the activity with lead backing y_{Pb}.

Bottom plot: influence of collimator diameter on the height h of the transition curve of photons responsible for $Cu^{63}(\gamma,n)Cu^{62}$ behind 2.7 s.u.

Figure 9 Beginning of transition curves of photons causing (γ,n) reactions on C and Cu using 330 Mev and 210 Mev bremsstrahlung.

Figure 10 Complete transition curves of photons causing (γ,n) reactions on C and Cu using 330 Mev and 210 Mev bremsstrahlung.

Figure 11 Beginning of transition curves of photons responsible for several reactions on Zn.

Figure 12 Complete transition curves in Pb of photons responsible for several reactions on Zn.

Figure 13 Transition curves in Pb of x-rays causing nuclear reactions in Ta.

Figure 14 Transition curves in Pb of x-rays causing nuclear reactions in Bi and Pb.

Figure 15 Bremsstrahlung spectrum as calculated for the Berkeley synchrotron.

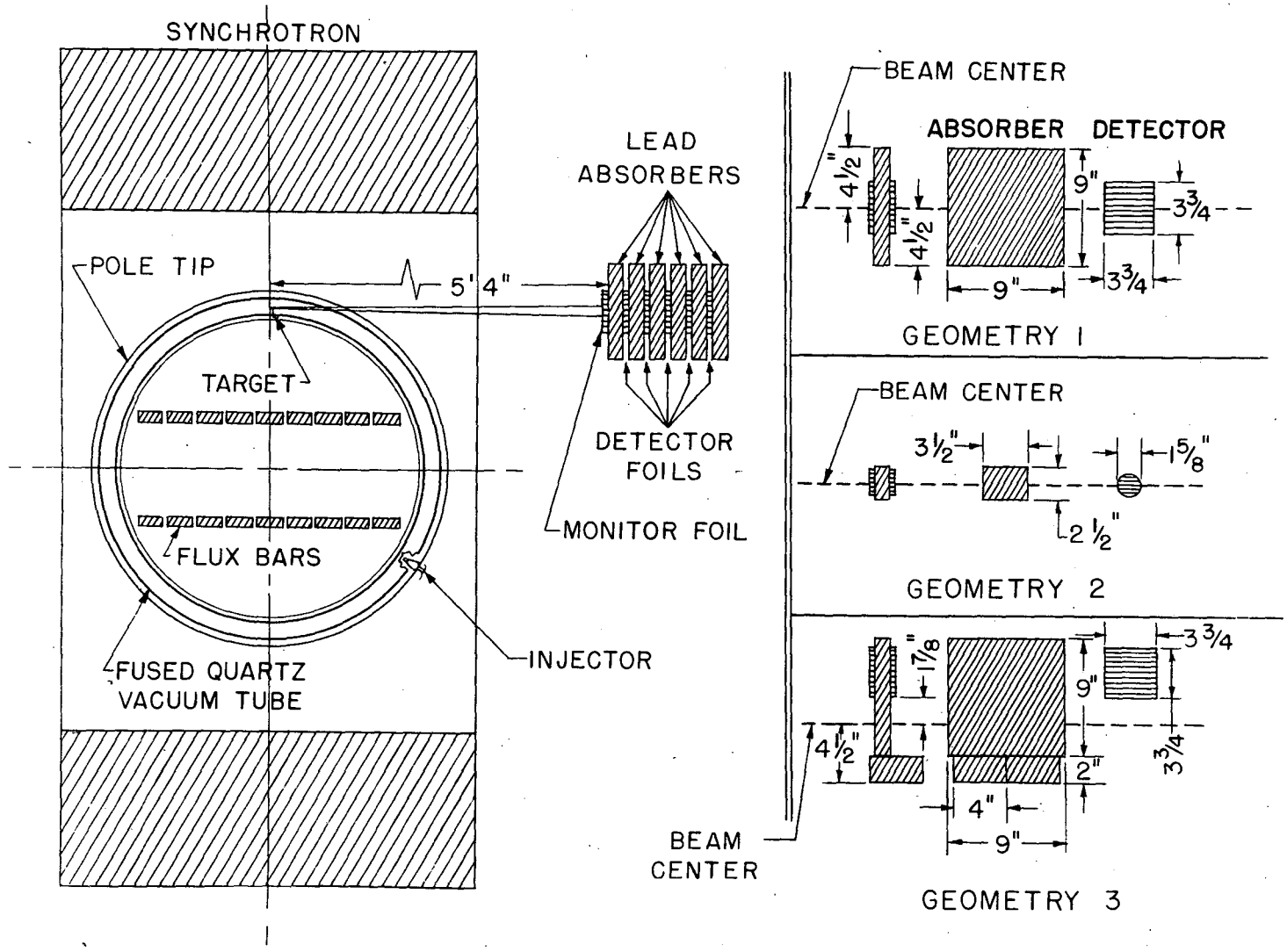
SYNCHROTRON
POLE TIP
5' 4"
TARGET
FLUX BARS
FUSED QUARTZ
VACUUM TUBE
INJECTOR
LEAD
ABSORBERS
DETECTOR
FOILS
MONITOR FOIL
BEAM CENTER
ABSORBER
DETECTOR
4½"
4½"
9"
3¾
9"
3¾
GEOMETRY 1
BEAM CENTER
3½"
1⅝"
2½"
GEOMETRY 2
1⅞"
3¾
9"
3¾
4½"
2"
4"
9"
BEAM
CENTER
GEOMETRY 3

FIG. 1

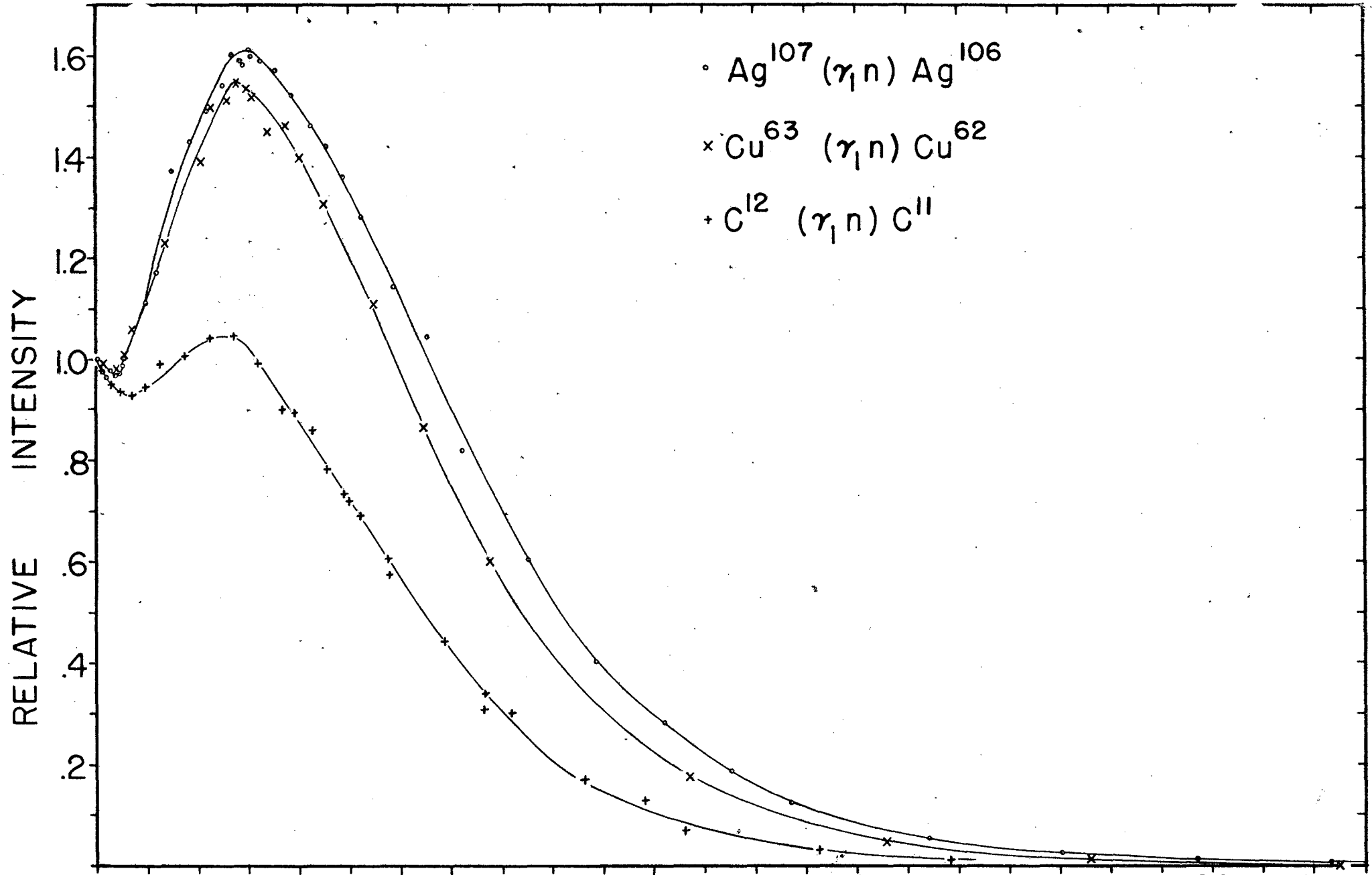

TRANSITION CURVES IN Pb OF X-RAYS CAUSING $(\gamma_1 n)$ REACTIONS

FIG. 2

14605-I

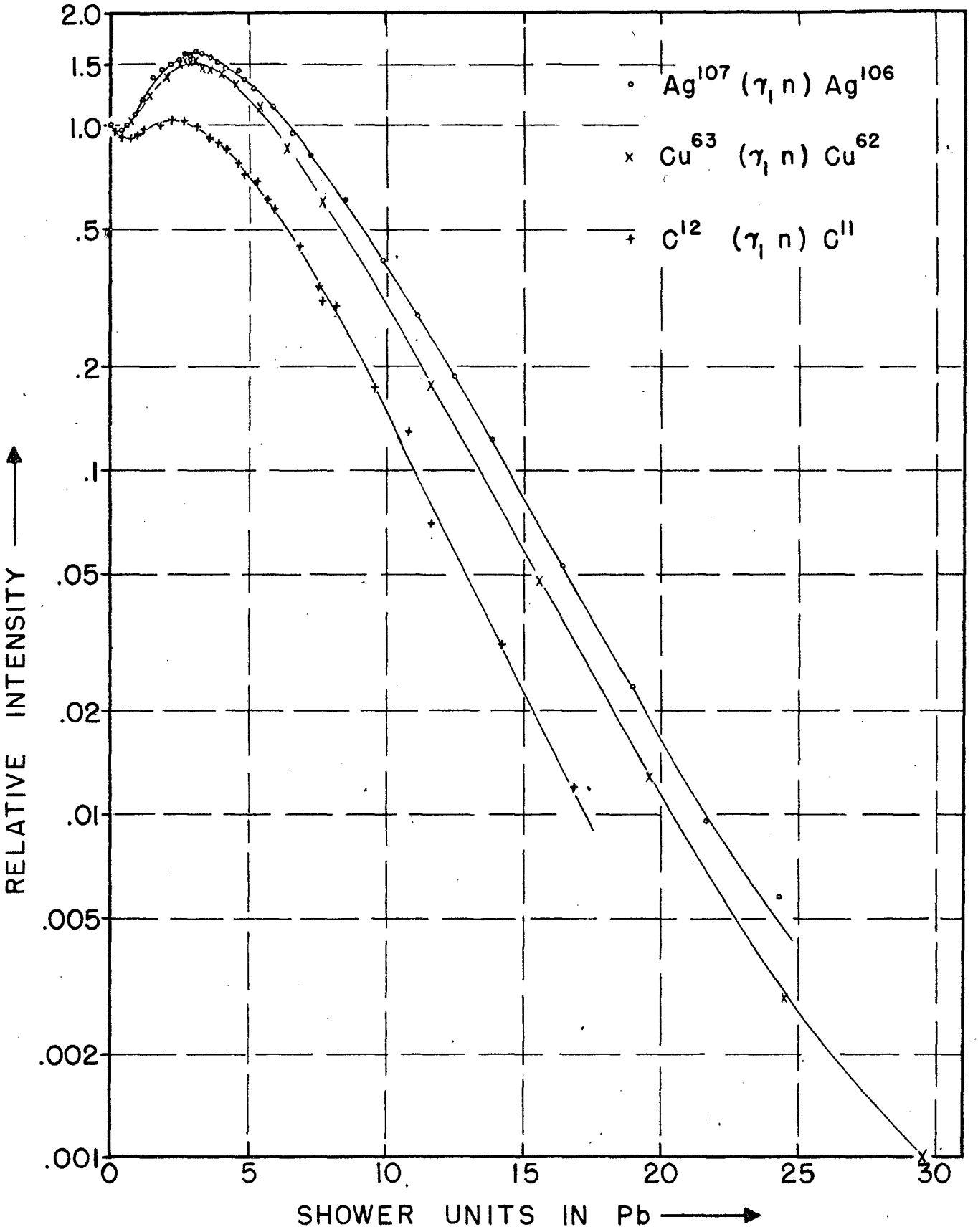

TRANSITION CURVES IN Pb OF X-RAYS CAUSING (γ_1 n) REACTIONS

FIG 3

14604-1

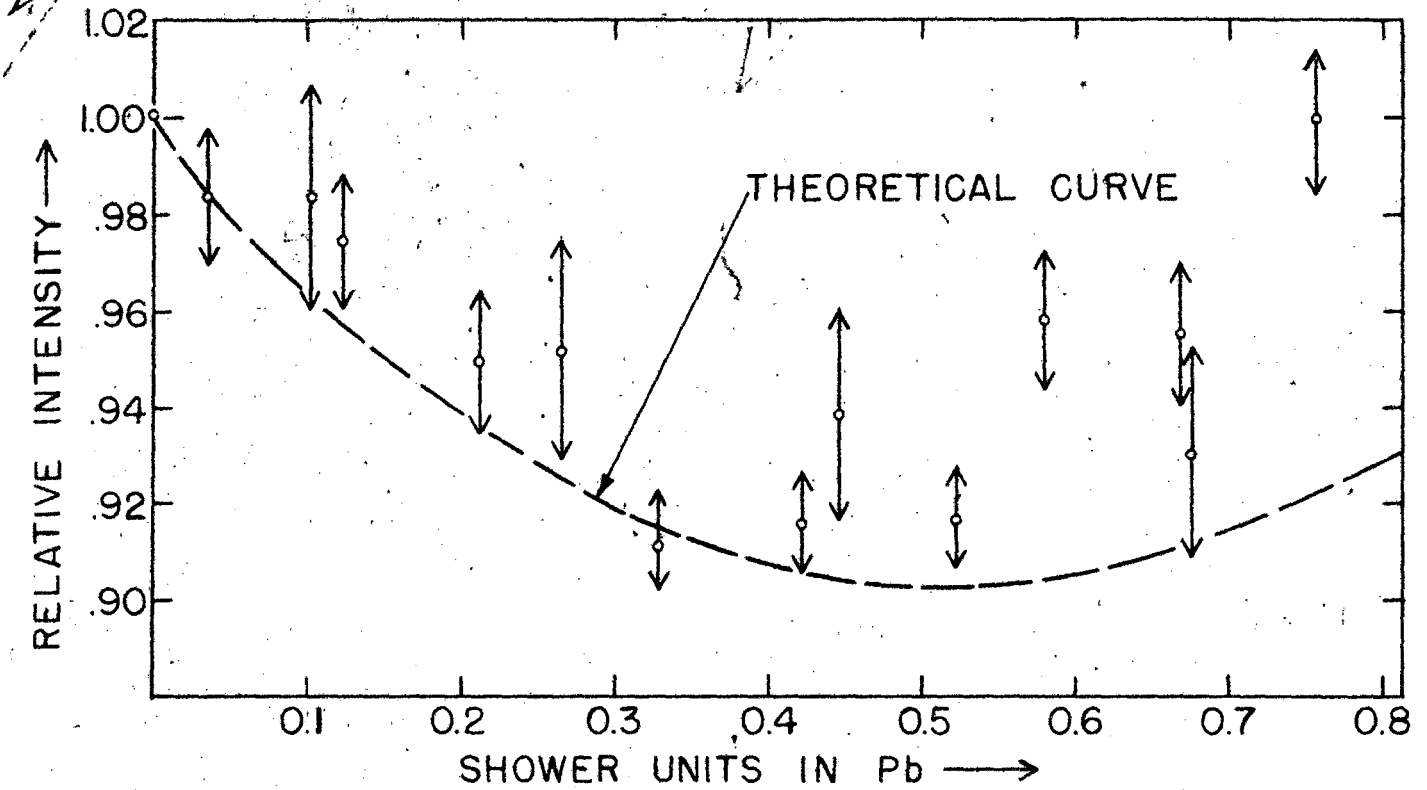

TRANSITION CURVE IN Pb OF X-RAYS CAUSING $C^{12}(\gamma, n)C^{11}$

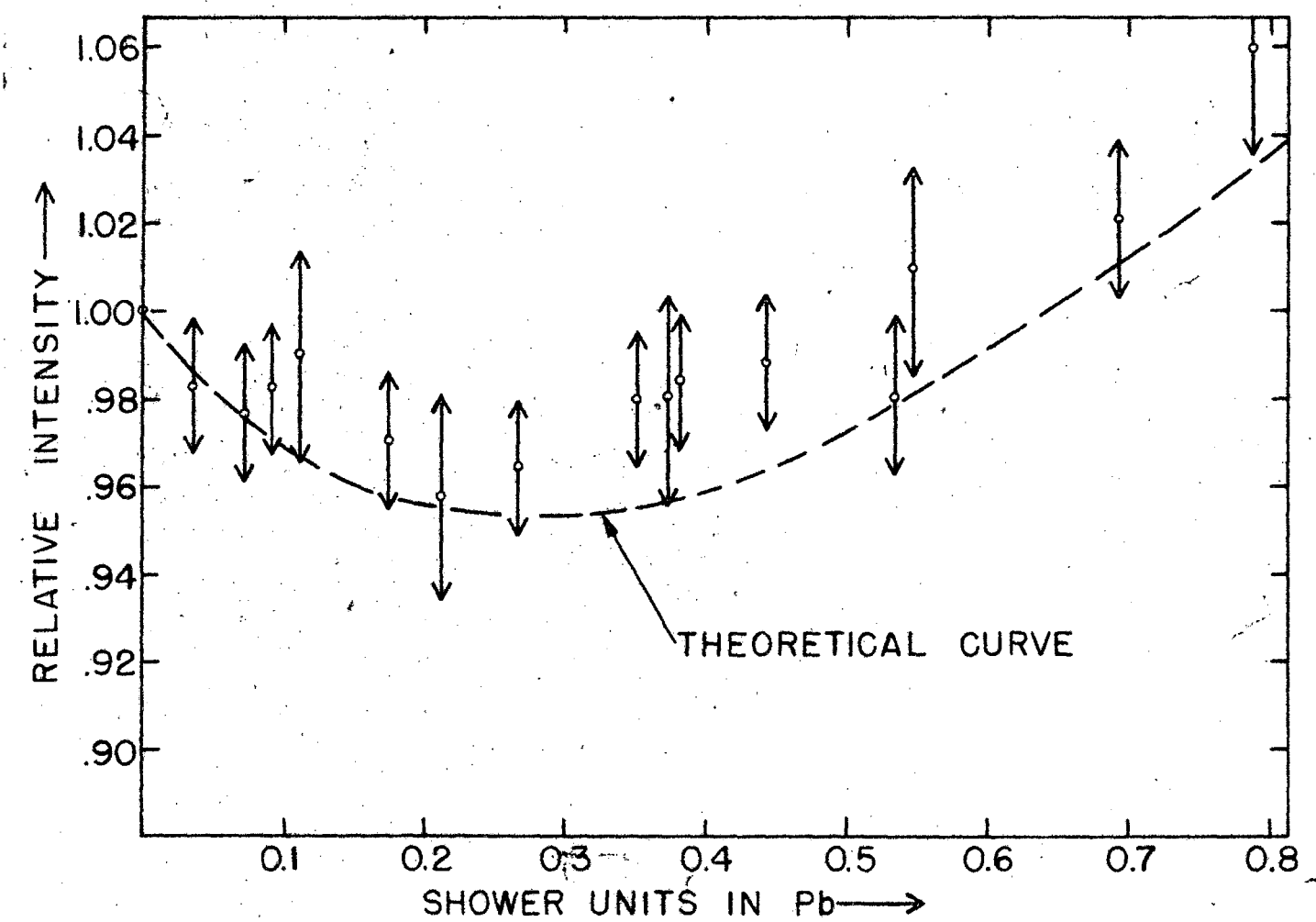

TRANSITION CURVE IN Pb OF X-RAYS CAUSING $Cu^{63}(\gamma,n)Cu^{62}$

Fig. 4

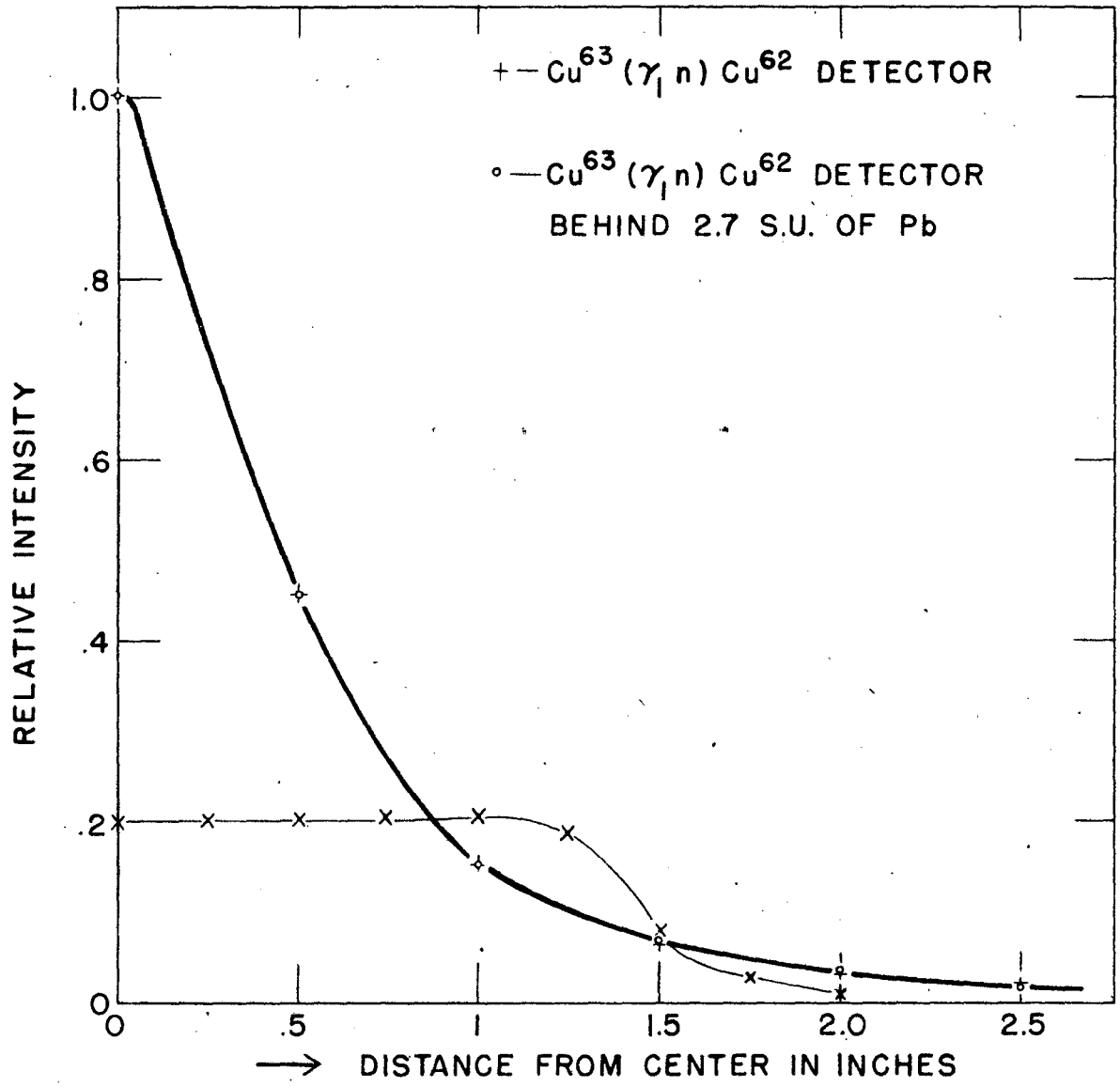

SYNCHROTON BEAM WIDTH AT 5 1/3 FEET FROM Pt. TARGET

FIG 5

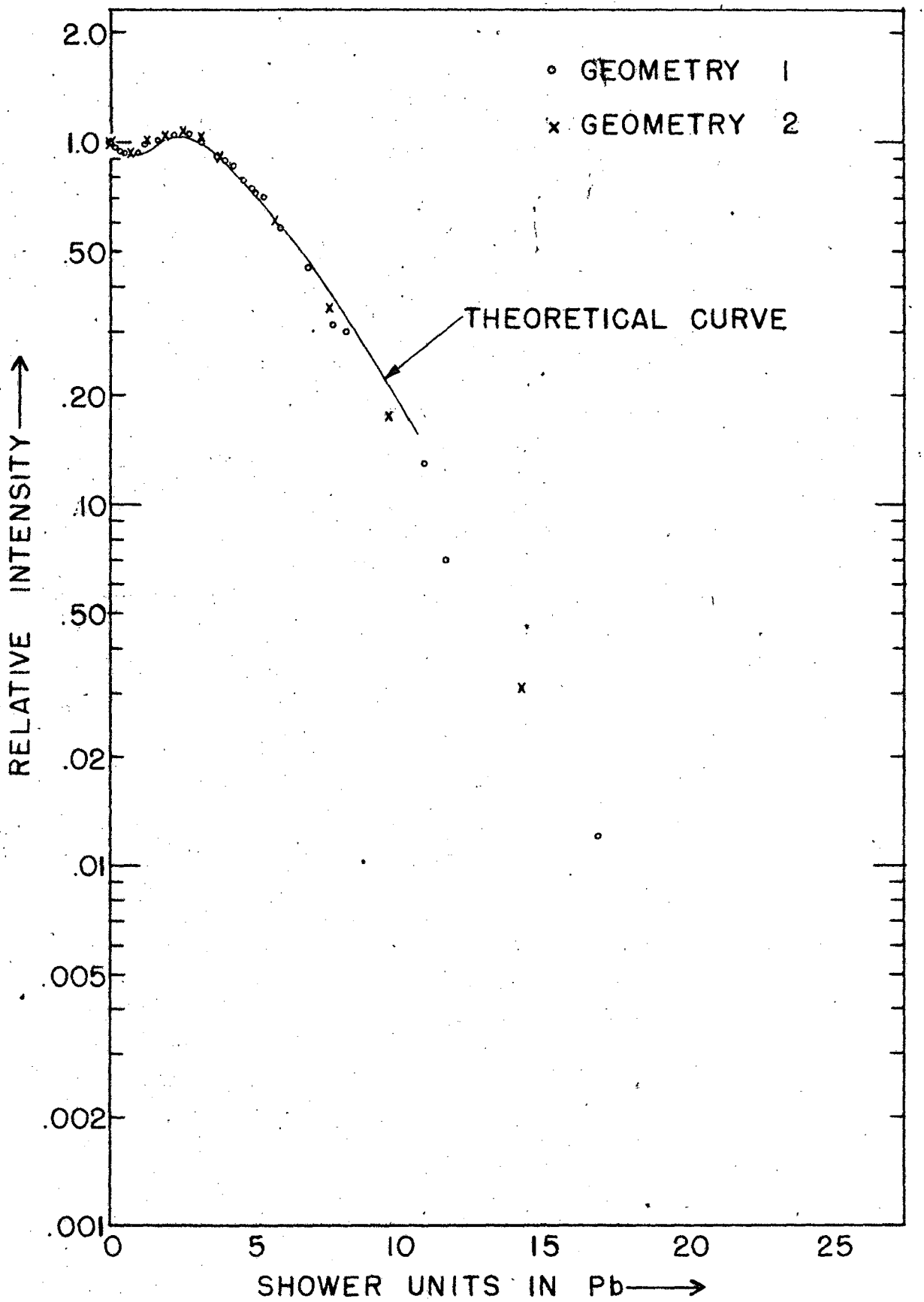

TRANSITION CURVE IN Pb OF X-RAYS CAUSING $C^{12}(\gamma, n)\, C^{11}$

Fig. 6

14933-1

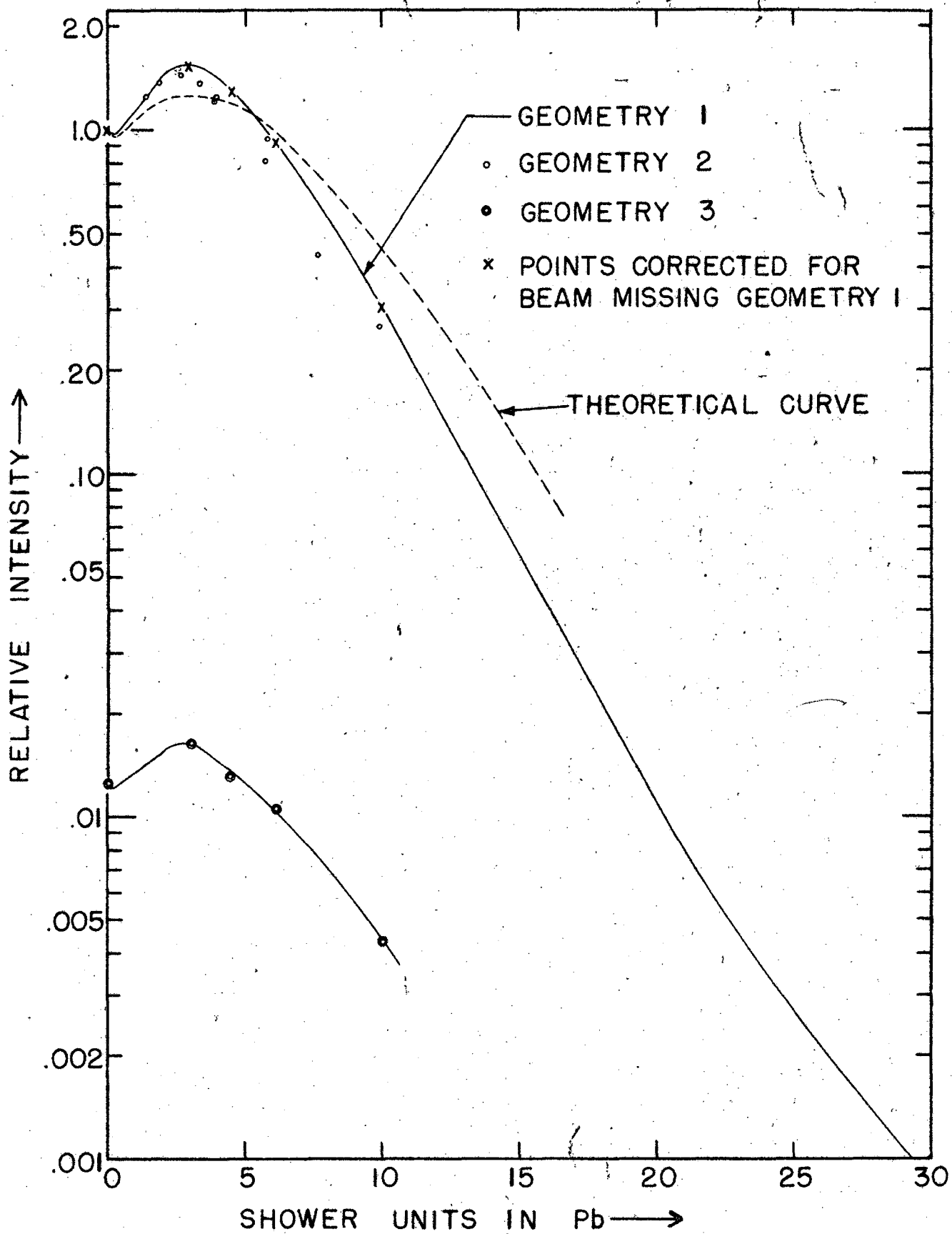

TRANSITION CURVE IN Pb OF X-RAYS CAUSING $Cu^{63}(\gamma, n)Cu^{62}$

14935-1

Fig. 7

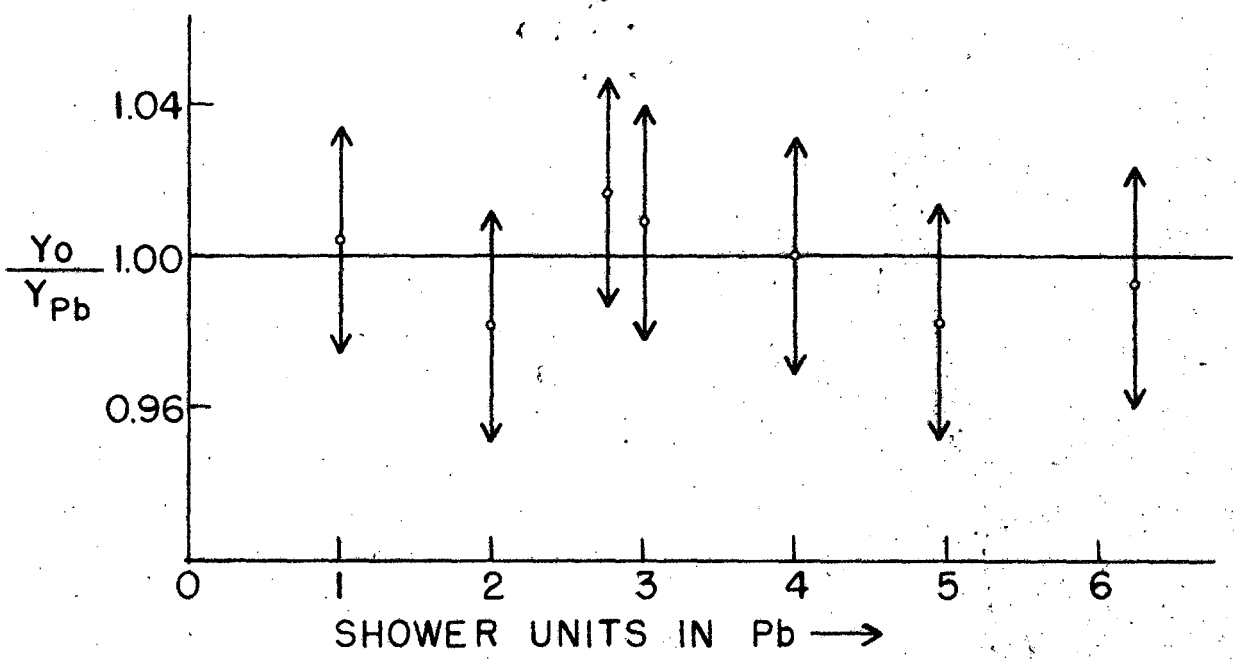
1.04
Yo / YPb
1.00
0.96
0
1
2
3
4
5
6
SHOWER UNITS IN Pb ⟶

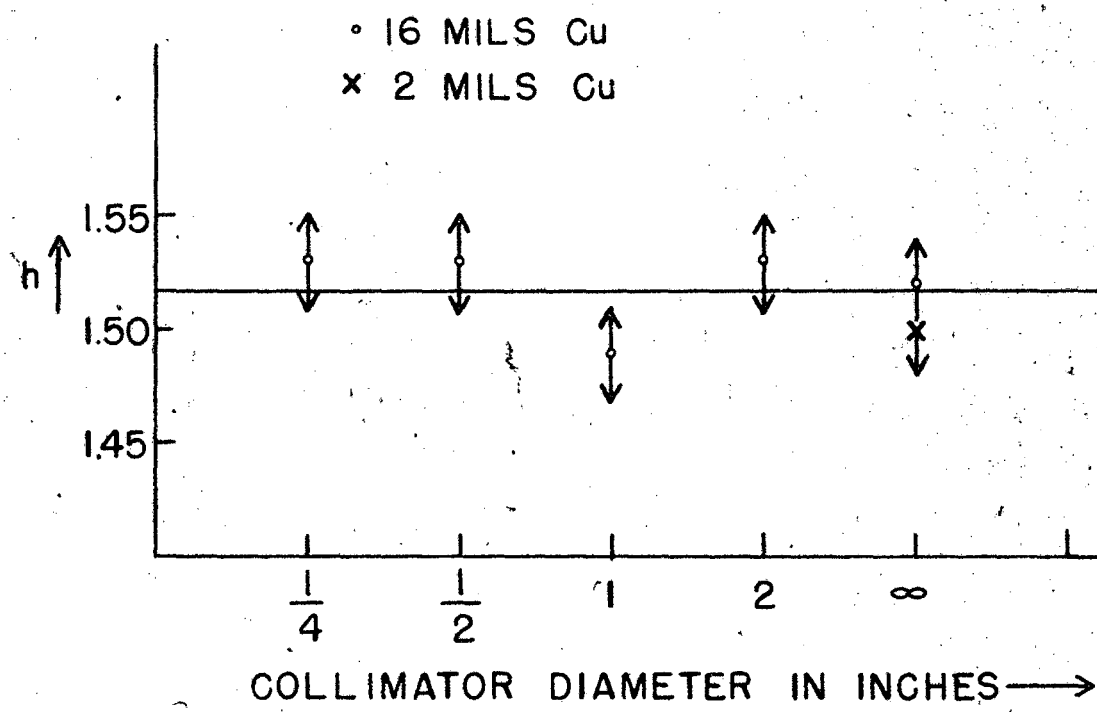
∘ 16 MILS Cu
× 2 MILS Cu
h
1.55
1.50
1.45
1/4
1/2
1
2
∞
COLLIMATOR DIAMETER IN INCHES ⟶

Fig. 8

14936-1

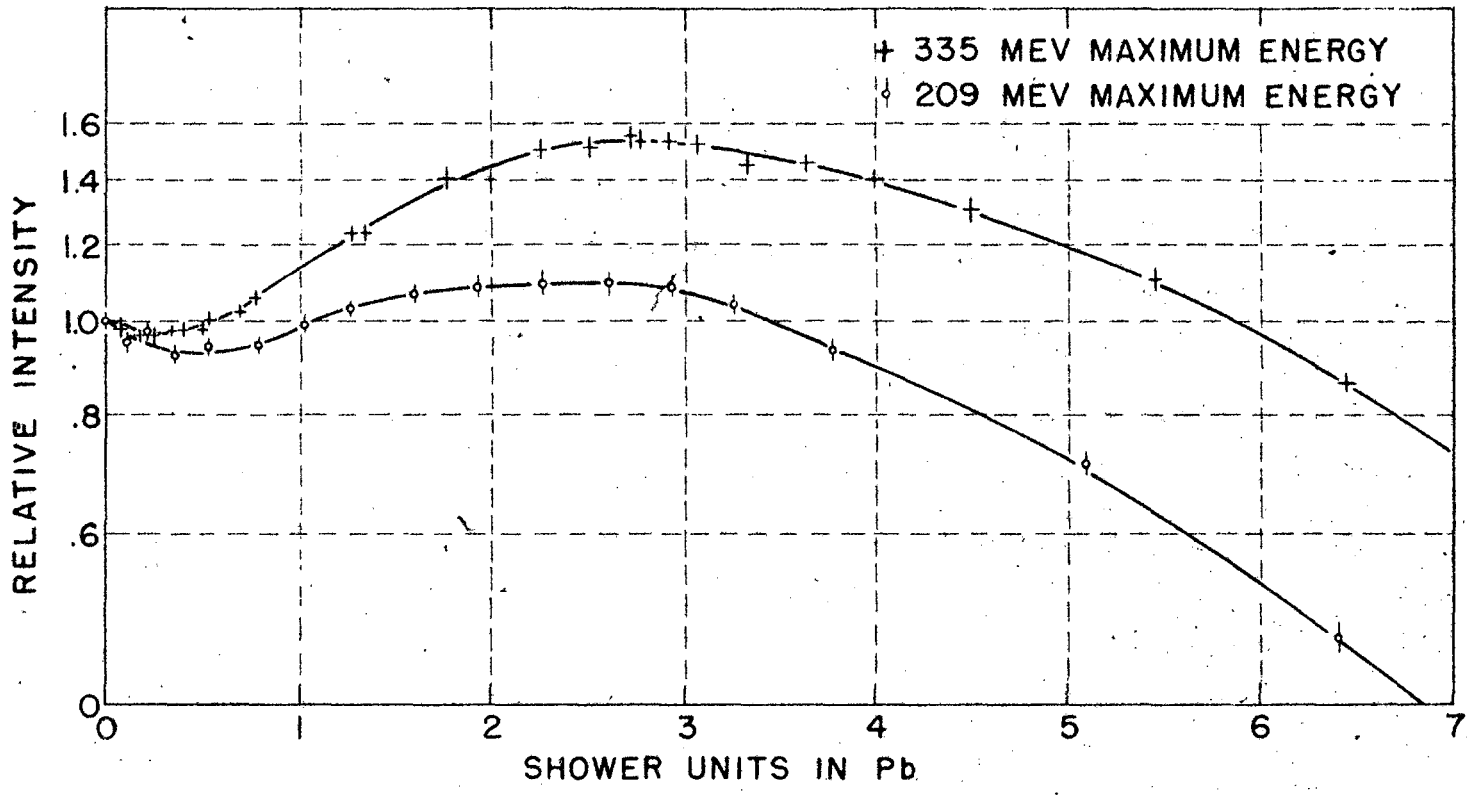

TRANSITION CURVE IN Pb OF X-RAYS
CAUSING Cu^{63} (γ, n) Cu^{62}

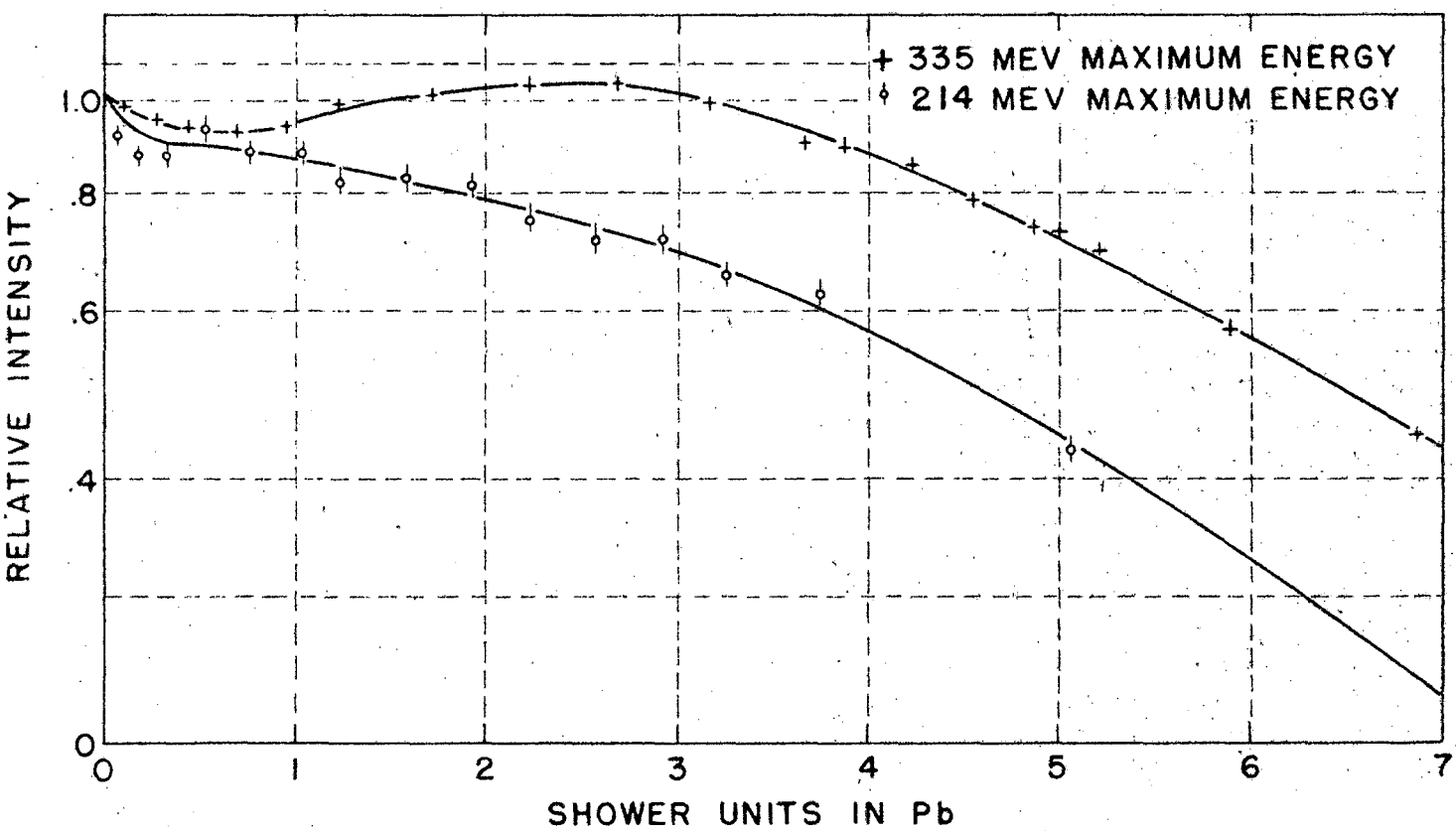

TRANSITION CURVE IN Pb OF X-RAYS
CAUSING C^{12} (γ, n) C^{11}

Fig. 9

14265-1

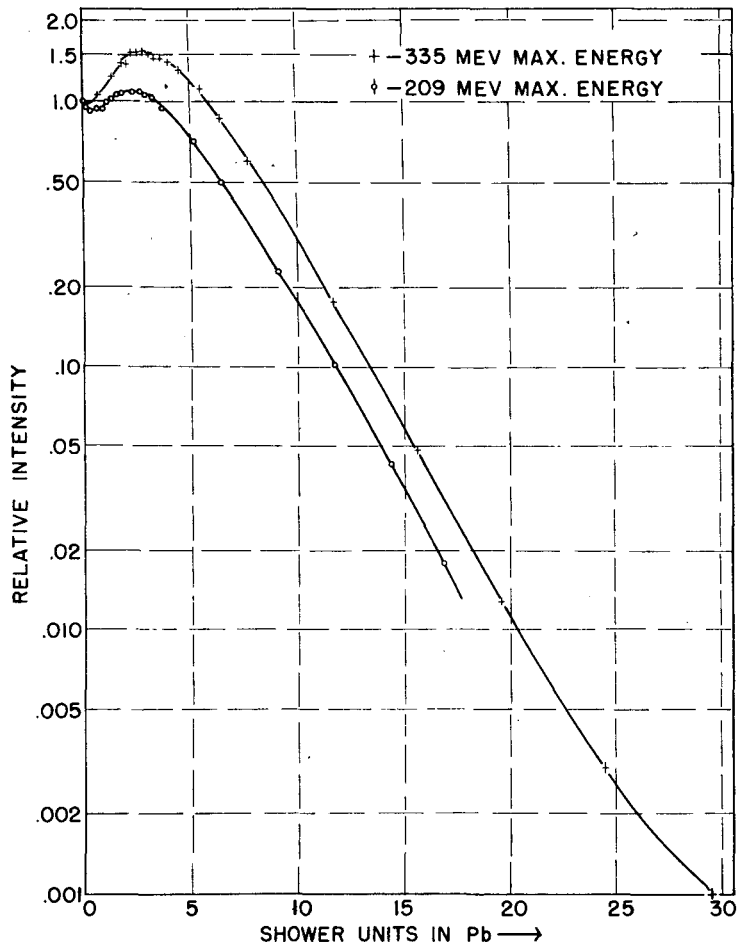

TRANSITION CURVES IN Pb OF X-RAYS CAUSING $Cu^{63}(\tau_1 n)\,Cu^{62}$

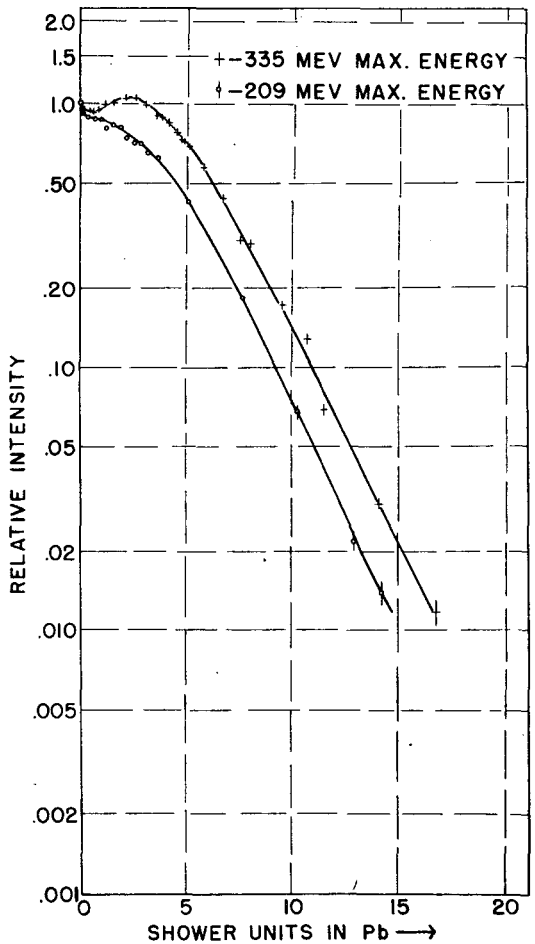

TRANSITION CURVES IN Pb OF X-RAYS CAUSING $C^{12}(\tau_1 n)\,C^{11}$

FIG. 10

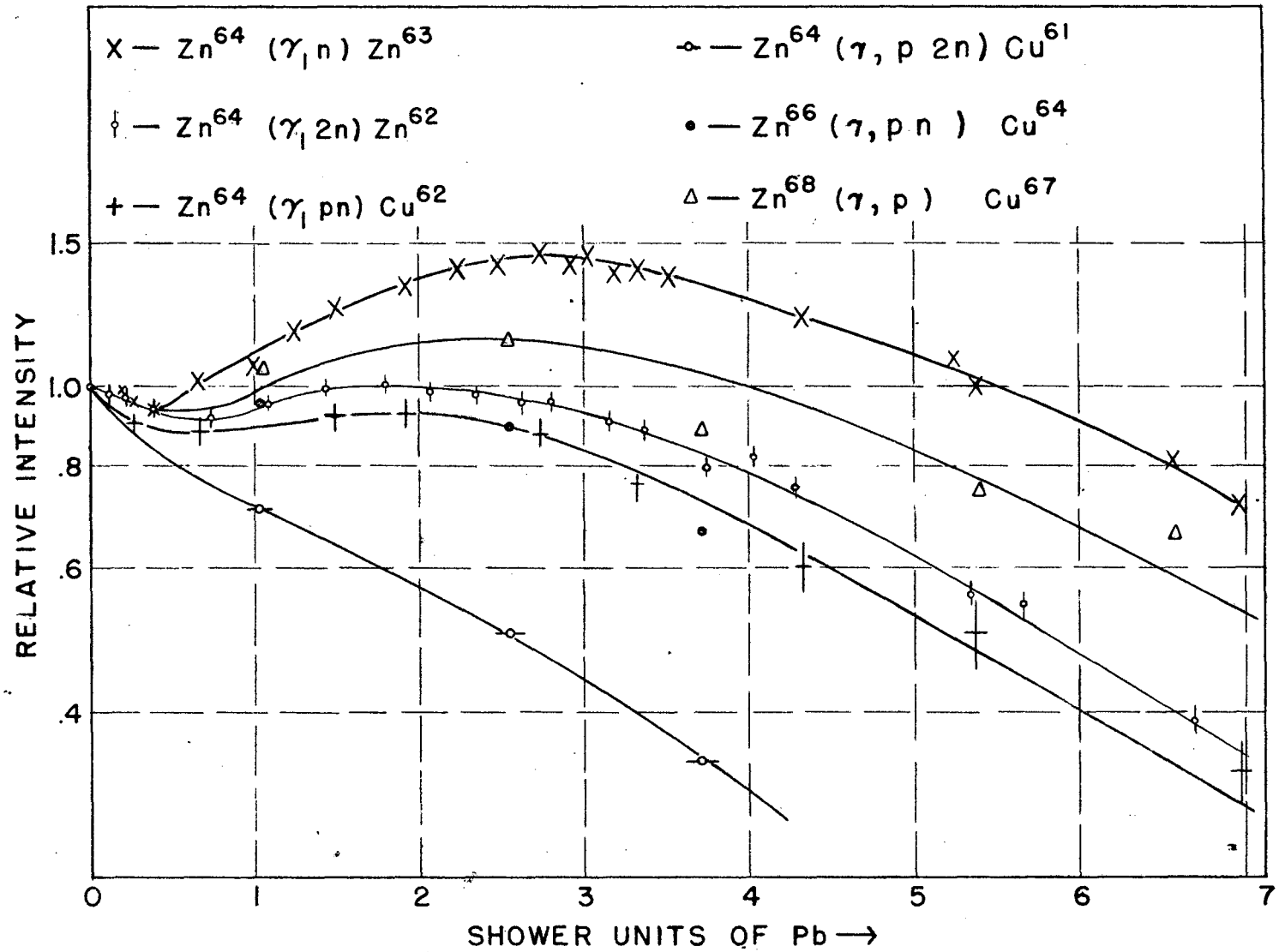

TRANSITION CURVES IN Pb OF X-RAYS CAUSING Zn REACTIONS

FIG 11

14263-1

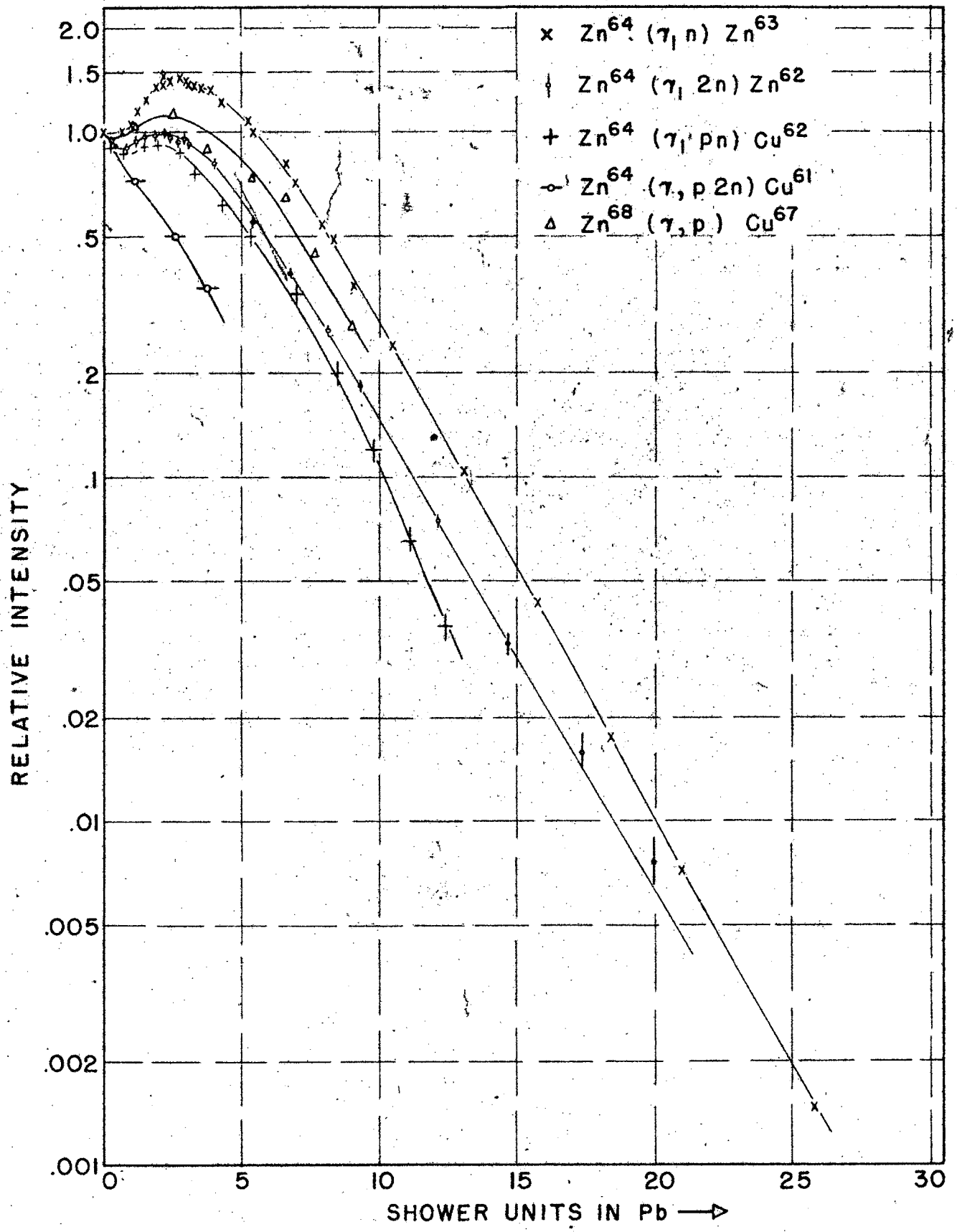

TRANSITION CURVES IN Pb OF X-RAY CAUSING NUCLEAR REACTIONS IN Zn.

Fig. 12

14388-1

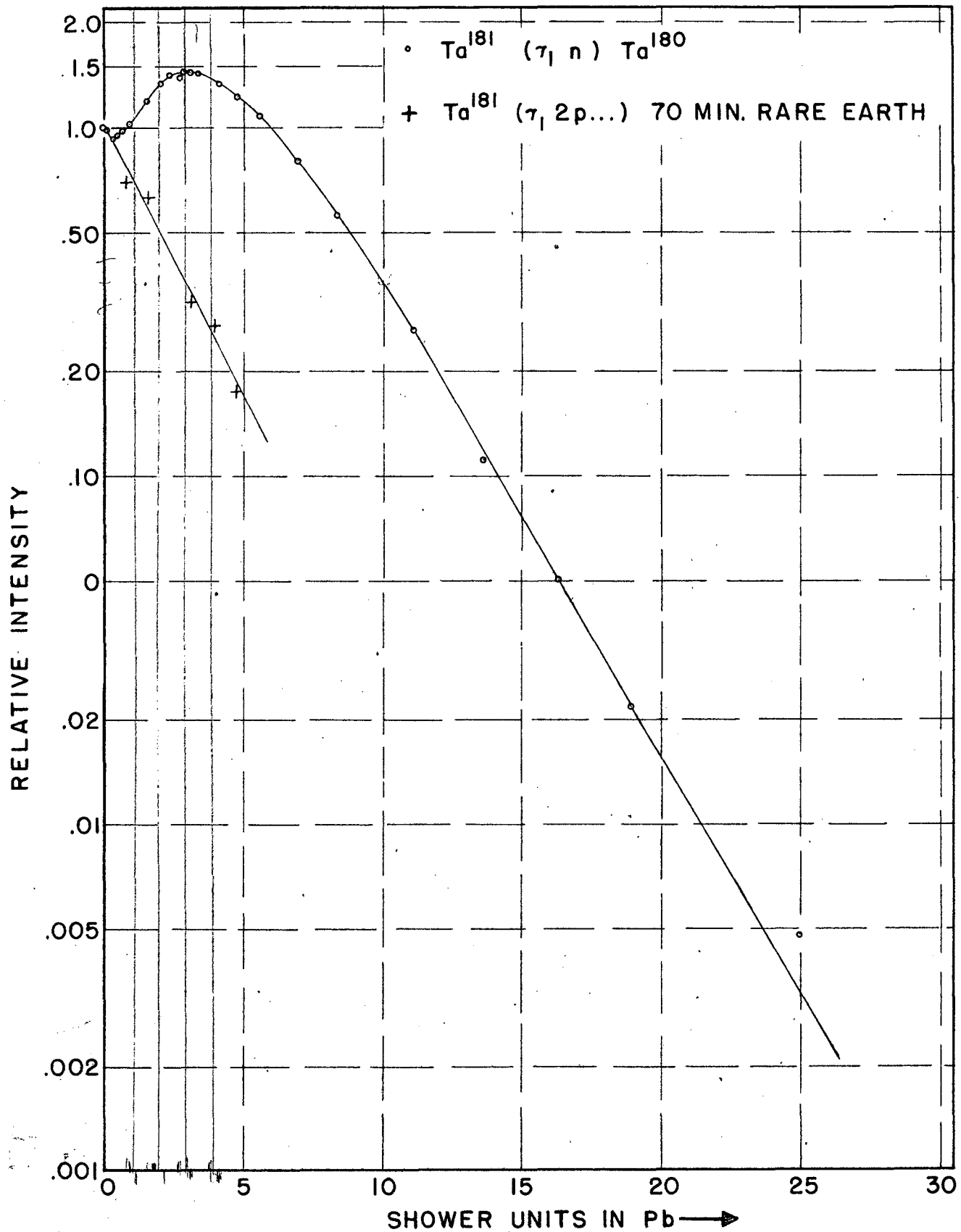

TRANSITION CURVES IN Pb OF X-RAY CAUSING NUCLEAR REACTIONS IN Ta.

FIG 13

14389-1

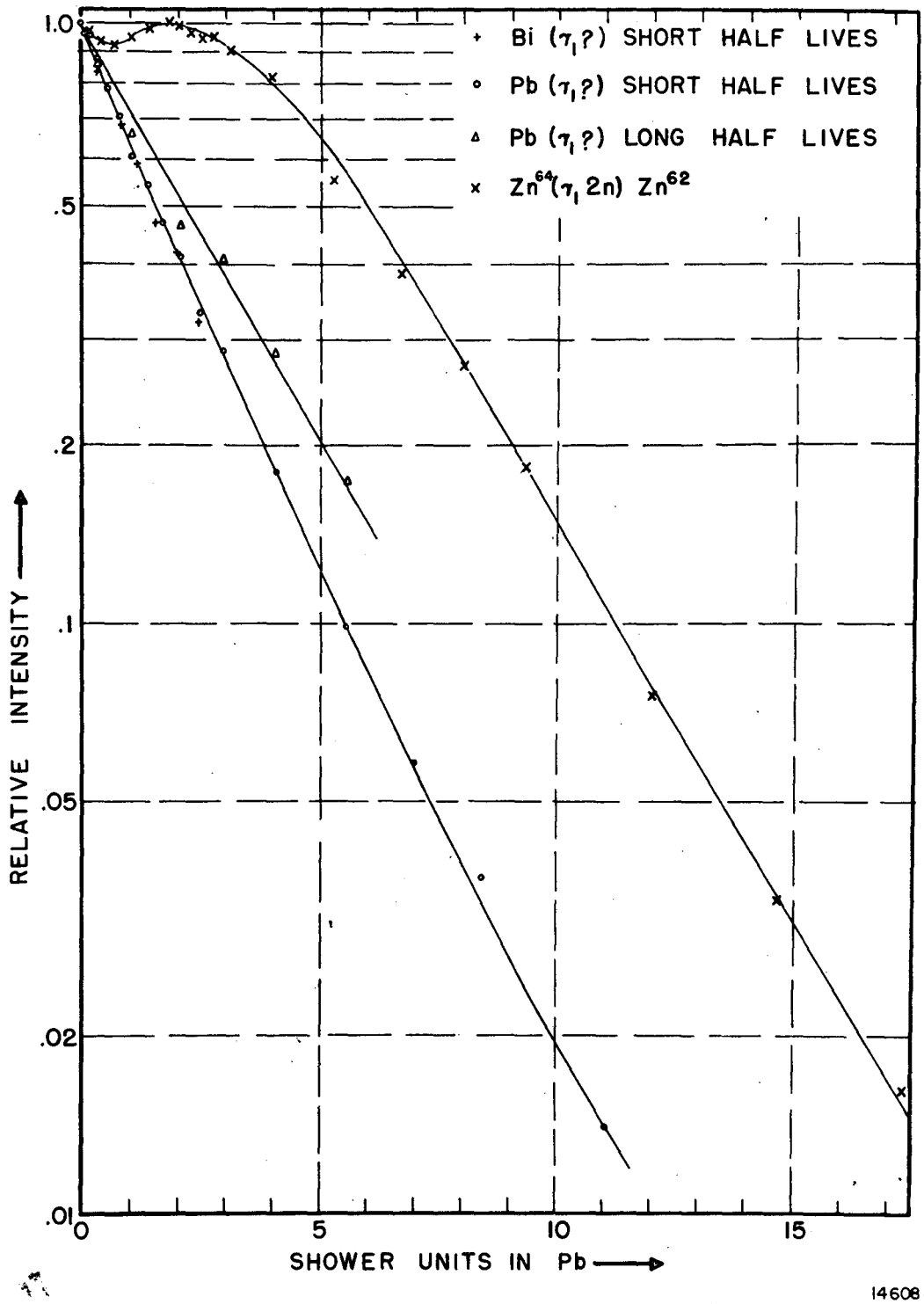

TRANSITION CURVES IN Pb OF X-RAYS CAUSING NUCLEAR REACTIONS IN Pb AND Bi.

FIG. 14

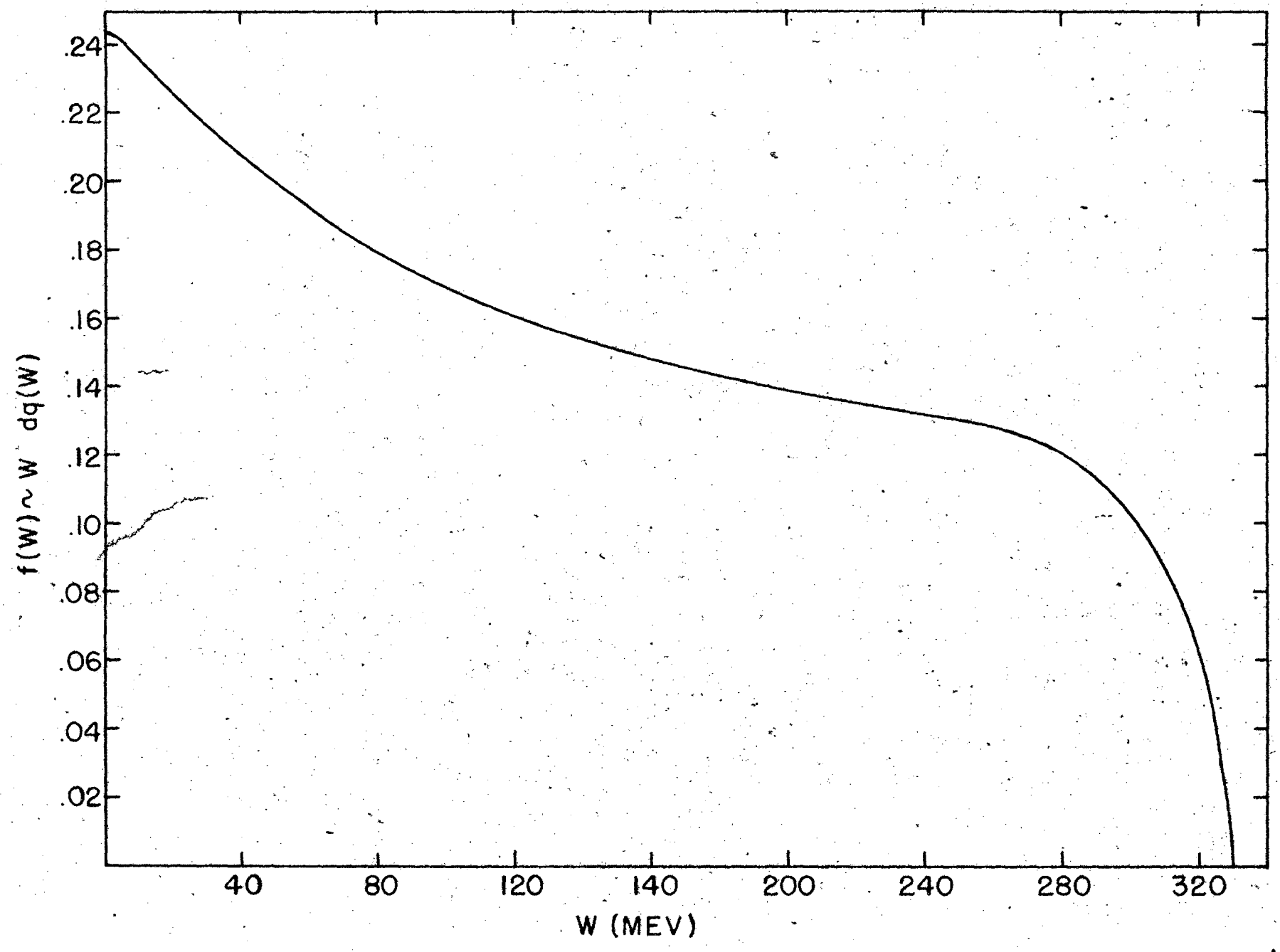

14937-1

Fig. 15

II. Nuclear Isomerism in Co^{58}

TABLE OF CONTENTS

1. Introduction

When a manganese metal target was bombarded with 40 Mev α-particles from the 60-inch cyclotron, a weak 8.8 hour activity appeared in the chemically separated cobalt fraction besides the expected long half lives of Co^{56} (72 days), Co^{57} (270 days) and Co^{58} (72 days). A similar period was found in cobalt fractions from nickel and cobalt bombarded with 18 Mev deuterons and fast neutrons, and from copper placed in the circulating deuteron beam of the 184-inch cyclotron. These cobalt samples were followed with a 3.2 mg/cm^2 end window Victoreen counter. When a 71 mg/cm^2 aluminum absorber was placed between the counter and the samples, no 8.8 hour activity could be detected; when a 210 mg/cm^2 absorber was used, the samples grew with a half life of approximately 9 hours. The results of the investigation reported here show this new period to be associated with an isomer of Co^{58}. The main part of the work was carried out with a magnetic lens spectrometer of the type described by Siegbahn,[1] calibrated with annihilation radiation.

2. Isotopic Assignment

The α-particle bombardment of manganese was found to be the most convenient method of production of the unknown activity: the only other period of comparable half-life formed in this case was the 2.6 hour Mn^{56}. The low measured intensity of the 8.8 hour activity made formation from target impurities suspect: a thorough chemical investigation* therefore had to be carried out and different manganese compounds in addition to the metal were used as targets. The bulk of the 8.8 hour activity under investigation followed the cobalt fractions and we can conclude that the new period belongs to that element.

The isotopic assignment is made by considering the momentum spectra of the cobalt fraction obtained from manganese bombarded with 40 Mev

---

* See Appendix

α -particles. This spectrum showed the characteristic radiations[2] of Co^{58}, Co^{57}, and Co^{56} formed by (α,n), (α,2n) and (α,3n) reactions. In addition a conversion line was found at 530 gauss cm which decayed with an 8.8 hour half-life; this corresponds to electrons whose range is only slightly larger than the 0.4 mg/cm^2 thickness of the nylon counter window. As will be seen in the next section, this line is due to L electrons, the K electrons being absorbed in the counter window. At the same time part of the continuous spectrum grew: an analysis showed the characteristic β^+ continuum of Co^{58} to be responsible for the growth. The activity associated with the conversion line thus decayed to Co^{58}.

Verification of this assignment was accomplished by reducing the α-energy to 17 Mev with aluminum absorbers, so that Co^{57} and Co^{56} (formed by (α,2n) and (α,3n) reactions were not present. The resulting spectrum is shown in Fig. 1. At low Bρ are two peaks due to K and L conversion electrons as obtained with a thin zapon window (cf. Section 3); in the center can be seen the continuous β^+ spectrum of Co^{58} that grew as the two low energy conversion peaks decayed (cf. Section 4); the insert at high Bρ magnifies the conversion electrons of the 805 Kev γ-ray of Fe^{58} (cf. Section 5). Any possible contamination by products of an (α,2n) reaction would have been noticed as conversion electrons of the 117 Kev and 130 Kev γ-rays emitted in the decay of Co^{57}; no such lines were observed. These results show the existence of an 8.8 hour isomer of Co^{58} decaying to the 72 day ground state.

3. Properties of the Isomer

In order to study the conversion electrons associated with the new isomer, a thin counter window was constructed with a single zapon film

supported by a wire grid. With the counter connected to a 2 liter reservoir, leakage was small enough so the counting characteristics did not appreciably change over 3 hour periods. This fact was checked by taking frequent counts with a standard. The cobalt sulfide sample, prepared from manganese bombarded with 17 Mev α -particles, was placed on a thin zapon film and was estimated to have less than 0.1 mg/cm^2 thickness. The observed K and L conversion peaks are shown in Fig. 1: the width at half maximum checks the known resolution of the spectrometer and the two lines are well separated. Possible M conversion electrons could not be resolved and are included under the L peak.

Since any small permanent $B\rho$ in the spectrometer is important at the low energies involved here, Auger electrons of Cd^{111} were used to check the calibration of the machine in this region. Values of 17.0 Kev and 24.1 Kev were obtained for the energies of the K and L cobalt conversion electrons; the $E_L - E_K$ difference of 7.1 Kev agrees within the expected error with the cobalt value of 6.9 Kev, and the energy of the isomeric transition is given as 24.9 Kev. The position of the L line was also measured by reversing the current and taking the average of the two values. The result was 24.2 Kev. The energy with estimated uncertainty of the isomeric transition is thus given as 24.9 $\pm$ 1.0 Kev. Considering this energy value and the half-life of 8.8 hours a $\Delta = 4$ transition is indicated according to Axel and Dancoff.(3)

The ratio of the K to L conversion coefficients has been obtained by comparing the intensity of the two lines. Lawson and Cork(4) have shown that the ratio of the experimental peak heights (before division of the counting rate by $B\rho$) should be equal to the ratio of the normalized areas (after division of the counting rate by $B\rho$). Experimental values given by these

two methods are shown in Table I. The close agreement indicates that self-absorption and back-scattering in the source, if not negligible, at least affect both peaks equally. That the thickness of the counter window did not appreciably influence the ratio was shown by placing zapon films prepared from the same solution as the window over the source. With one film covering the sample a decrease of 2 percent in the relative peak height was observed; with two films this decrease amounted to 7 percent. The contribution of M electrons to the L peak is unknown but believed small. Table I also lists theoretical values for a $\Delta = 4$ transition obtained from the paper by Hebb and Nelson.(5) The isomeric transition thus appears due to a mixture of magnetic 2^3 and electric 2^4 pole radiation.

The 72 day decay of the ground state of Co^{58} has been investigated by Deutsch and co-workers.(6)(7) They have shown that the decay proceeds 14.5 percent by β^+ emission and 85.5 percent by K capture to an excited state of Fe^{58} from which the ground state is reached by emission of an 805 Kev γ-ray. The β^+ spectrum has an end point of 0.47 Mev. It is concluded that the β^+ transition occurs with an angular momentum change of one or zero, with the parity change undetermined. No decay to the ground state of Fe^{58} was observed by these investigators, which means that this transition must be at least twice forbidden by comparison with Co^{56} whose decay has this degree of forbiddenness according to Konopinski.(8)

No evidence for the decay of the isomer of Co^{58} to the ground state of Fe^{58} was found: this would have appeared as high energy β^+ particles decaying with the 8.8 hour half-life. Transitions from the isomer to the excited state of Fe^{58} would have been hard to detect due to the small energy difference between the two states of Co^{58}; however, such transitions must be very rare as indicated in the following section.

4. Relative Cross Section

During the bombardment of a thick manganese target with 17 Mev α-particles both 8.8 hour isomeric and 72 day ground state of Co^{58} are formed. The continuous β^+ spectrum grows therefore as the isomer decays after the sample is introduced into the spectrometer. This was observed by following the activity at the $B\rho$ = 1500 gauss cm point with time; since the length and intensity variation of the bombardment is known, the ratio of the cross section for the formation of the isomer σ_1 to the cross section for formation of the ground state σ_2 can be calculated and a value of $\sigma_1/\sigma_2 = 1.7$ is obtained. The result would be in serious error if an appreciable number of transitions occurred between the isomer and the excited state of Fe^{58}. This is highly improbable since even if such a transition were of the allowed or first forbidden type it would have a partial half-life comparable to the 72 days of the ground state; however possible spin assignments discussed in Section 6 make such a decay very highly forbidden.

5. Conversion Coefficient of the Fe^{58} γ-Ray

The conversion electrons of the 805 Kev γ-ray emitted following emission by the ground state of Co^{58} are shown in the insert of Fig. 1. A relatively thick source of about 1 mg/cm^2 and a 0.4 mg/cm^2 nylon counter window were used to measure the β^+ continuum and the high energy conversion line in order to obtain large enough counting rates. The continuous background between the end of the β^+ spectrum and the 805 Kev line was probably due to Compton electrons from the source and parts of the spectrometer. The width at the half intensity point of the line agrees with the known 4 percent resolution of the spectrometer; however the maximum counting rate on the peak was only twice the normal counter background. This makes the result sensitive to inevitable background variations. The contribution from photo-

electrons produced in the sample should amount to only a few percent. To check on this possible source of error a 2.8 mg/cm^2 nickel foil was placed over the source and no significant change in peak height observed.

To obtain the desired conversion coefficient the ratio of the area under the line to 6.9 times the area under the continuous β^+ spectrum must be taken. The latter is distorted below 150 Kev by scattering in the sample and counter window. Above this energy a Fermi plot gives a straight line. This line was extrapolated to 0 momentum and the result used to obtain the area under the β^+ spectrum. The conversion peak contains both K and L electrons. According to Hebb and Nelson[4] the latter amount to 8 percent of the total number. This correction was applied to the observed area under the line. Thus the value quoted in Table II is obtained.

This table also lists theoretical values of the conversion coefficient as interpolated from recent calculations by M.E. Rose.[9] Comparison with the experimental result indicates a magnetic dipole transition, although the estimated accuracy of the measurement is not such as to exclude electric quadrupole radiation. In either case the transition occurs with no change in parity.

6. Discussion

Fig. 2 represents a decay scheme of Co^{58} possible on the basis of the results of Deutsch et al.[6][7] summarized in Section 3 and the work reported in this paper. The spin of the ground state of Fe^{58}, an even-even nucleus, is undoubtedly 0 and the parity was taken + on the basis of the shell model. The spin and parity assignments in Fig. 2 are made by assuming the β^+ decay of Co^{58} to be of the "allowed" type and appear the only possible ones if the excited Fe^{58} state decays by magnetic dipole radiation. If electric quadrupole radiation is responsible for this transition, then the assignments for

the 0.805 Mev, 1.785 Mev, and 1.810 Mev levels could be 2+, 2+ and 5+, or 2+, 3+ and 6+ respectively. Values of 2+, 3− and 6− for these levels appear probable if a first forbidden transition is responsible for the β^+ spectrum. In any case the isomeric state has a higher spin value than the ground state.

This is verified by the measured relative cross sections for formation of the two states of cobalt. According to the statistical theory this is given by $\sigma_1/\sigma_2 = \frac{2I_1 + 1}{2I_2 + 1}$, where σ_1 and σ_2 are the cross sections for the formation and I_1 and I_2 the spin values of the isomeric and ground states respectively. This formula is only expected to apply to the case of high excitation energy and heavy nuclei as discussed by Segrè and Helmholz.[10] As was just seen, two sets of choices for I_1 and I_2 appear possible: they give theoretical values for the relative cross section of 2.20 and 1.86. These are close to the experimental result of $\sigma_1/\sigma_2 = 1.7$.

It is of interest to compare the properties of the isomers of Co^{58} and Co^{60}. The latter has been investigated by Deutsch, Elliot and Roberts[11] and more recent work is quoted by Axel and Dancoff.[3] From these the following conclusions can be drawn:

(1) The Co^{60} isomer decays to the ground state by emission of a mixture of 2^3 magnetic and 2^4 electric pole radiation; this is similar to Co^{58} as shown in Section 3. Thus the same spin difference exists between the two levels of each isotope.

(2) The spin I_1 of the isomeric state in Co^{60} is lower than the spin I_2 of the ground state; the opposite is true for Co^{58}. It is possible that corresponding spin values are the same for the two isotopes, but this cannot be ascertained from the available data. The reversal of the spin order might indicate a crossing of energy levels as two neutrons are added to Co^{58}.

7. Acknowledgments

The writer is greatly indebted to Professor A.C. Helmholz for his continued interest and many helpful suggestions during the course of this work. The β-ray spectrometer was constructed by Dr. R. W. Hayward and its use is much appreciated. Mrs. D. Stewart suggested several of the chemical separations. Thanks are also due Mr. Bernie Rossi and the 60-inch cyclotron crew for carrying out the bombardments.

Appendix: Chemical Procedure

To the solution of Mn in HCl 10 mg amounts of Co, Cu, Fe, Ni, Zn carriers were added. The 1N solution was saturated with $(NH_4)_3SCN$ and shaken with a 50 percent mixture of diethyl ether and amyl alcohol. After several washings the alcohol-ether extract was found to be free of Mn. The remaining metals were removed from the extract by shaking with an ammoniacal solution, the copper precipitated as sulfide in .3N acid solution, the nickel separated as the dimethyl glyoxime, the zinc obtained as sulfide in nearly neutral solution, the iron precipitated as the hydroxide and finally the cobalt separated as sulfide in a basic solution or precipitated by nitroso-β-naphthol. This procedure in parts or as a whole was repeated several times. After the assignment to the element had been established, 1 mg amounts of Co carrier were extracted from a solution of the manganese target with the alcohol-ether mixture, and directly precipitated as the sulfide from an ammoniacal solution.

Table I

Experimental and theoretical values for a $\Lambda = 4$ transition of the ratio of the conversion coefficients in the K and L shells for the 24.9 Kev γ-ray of Co^{58}.

Experiment		Magnetic 2^3 pole	Electric 2^4 pole
from peak heights	from area		
$1.93 \pm .10$	$1.89 \pm .19$	6.6	.41

Table II

Experimental and theoretical values of the internal conversion coefficient in the K shell for the 805 Kev γ-ray of Fe^{58}: $a_K \times 10^4$

Experiment	Electric pole		Magnetic pole	
	2^1	2^2	2^1	2^2
2.5	1.3	3.4	2.4	5.9

FIGURE CAPTIONS

Figure 1 Momentum spectrum of β-particles emitted by both isomeric and ground states of Co^{58}.

Figure 2 Proposed decay scheme of Co^{58}.

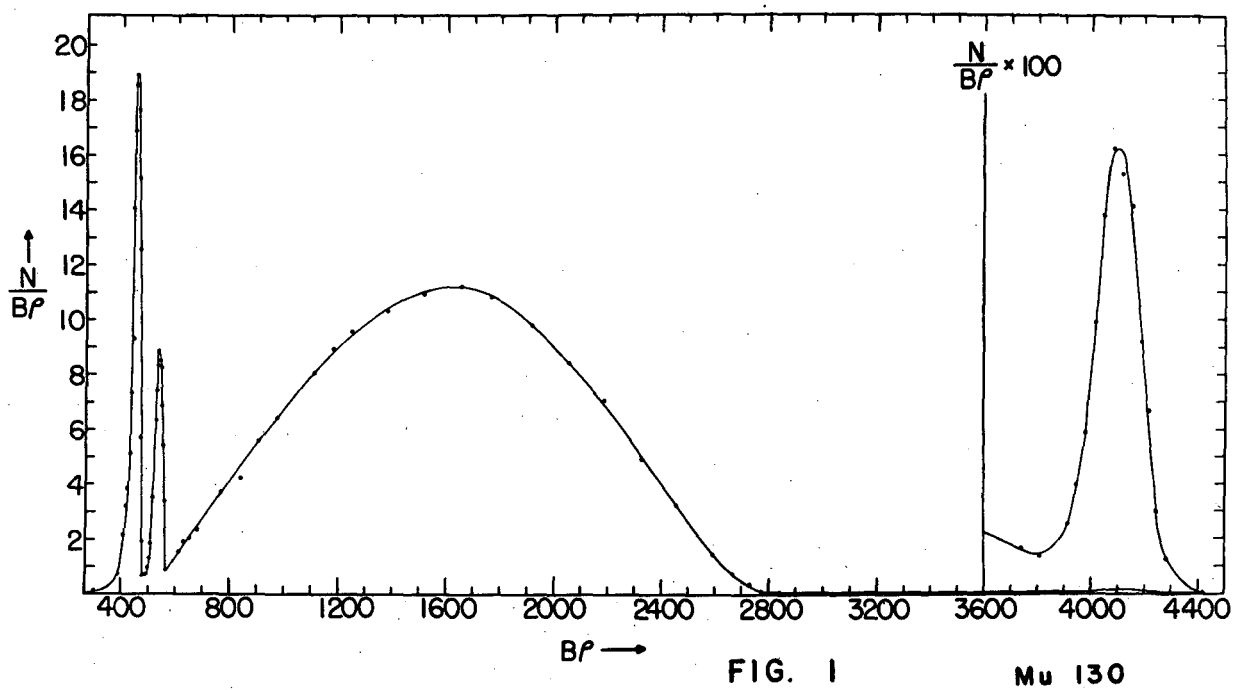
N/Bρ
20
18
16
14
12
10
8
6
4
2
400
800
1200
1600
2000
2400
2800
3200
3600
4000
4400
Bρ →
N/Bρ × 100

FIG. 1 Mu 130

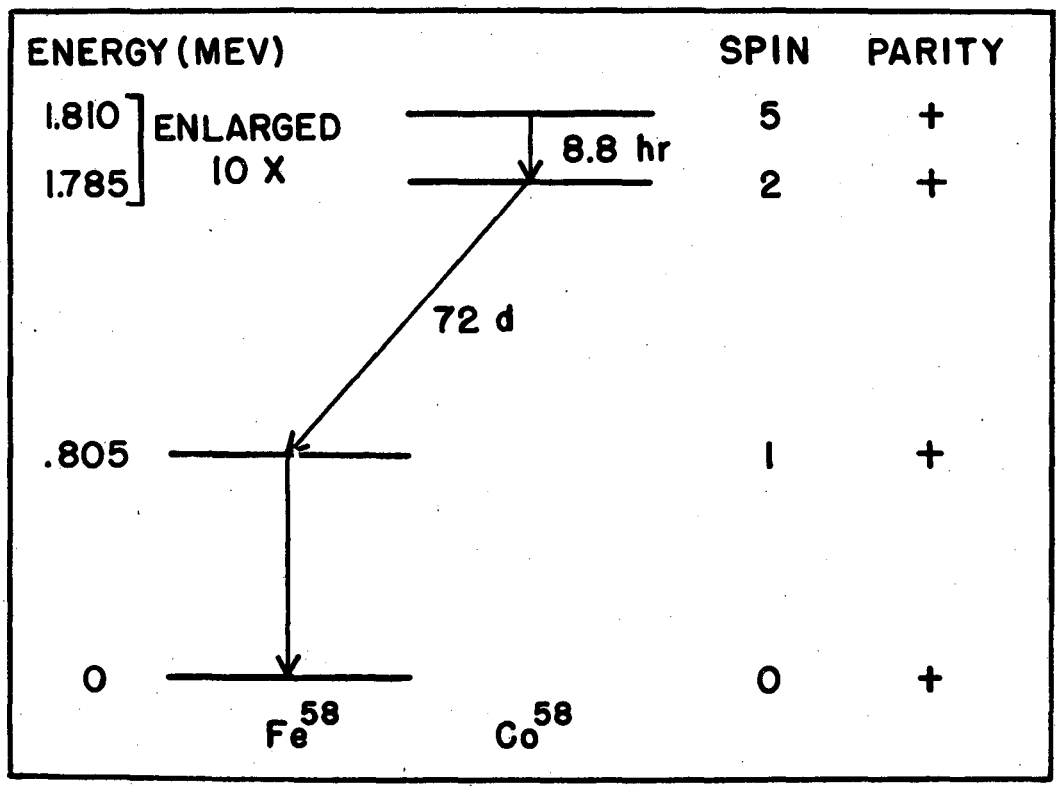
ENERGY (MEV)
SPIN
PARITY
1.810
1.785
ENLARGED
10 X
8.8 hr
5
+
2
+
72 d
.805
1
+
0
0
+
Fe58
Co58

FIG. 2

Mu 131

BIBLIOGRAPHY

(1) J. K. Siegbahn, Phil. Mag. 37, 162 (1946)

(2) G. T. Seaborg and I. Perlman, Rev. Mod. Phys. 20, 585 (1948)

(3) P. Axel and S. M. Dancoff, Phys. Rev. 76, 892 (1949)

(4) J. L. Lawson and J. M. Cork, Phys. Rev. 57, 982 (1940)

(5) M. H. Hebb and E. Nelson, Phys. Rev. 58, 486 (1940)

(6) M. Deutsch and L. G. Elliot, Phys. Rev. 65, 211 (1944)

(7) W. M. Good, D. Peaslee and M. Deutsch, Phys. Rev. 69, 313 (1946)

(8) E. J. Konopinski, Rev. Mod. Phys. 15, 209 (1943)

(9) M. E. Rose et al., "Low Z internal conversion coefficients," privately circulated

(10) E. Segrè and A. C. Helmholz, Rev. Mod. Phys. 21, 271 (1949)

(11) M. Deutsch, L. G. Elliot and A. Roberts, Phys. Rev. 68, 193 (1945)